Critical Reviews in Biochemistry and Molecular Biology, 38:351–384, 2003

ISSN: 1040-9238
DOI: 10.1080/10409230390242380

Nitrogen Fixation: The Mechanism of the Mo-Dependent Nitrogenase

Robert Y. Igarashi and Lance C. Seefeldt

Department of Chemistry and Biochemistry, Utah State University, Logan, UT 84322, USA

ABSTRACT: This review focuses on recent developments elucidating the mechanism of the Mo-dependent nitrogenase. This enzyme, responsible for the majority of biological nitrogen fixation, is composed of two component proteins called the MoFe protein and the Fe protein. Recent progress in understanding the mechanism of this enzyme has focused on elucidating the structures of the active site metal clusters and of the proteins, understanding substrate interactions with the active site, defining the flow of electron transfer between the metal clusters, and defining the various roles of MgATP hydrolysis.

KEYWORDS: Nitrogen cycle, metalloenzyme, MgATP, electron transfer, FeS cluster

TABLE OF CONTENTS

I. INTRODUCTION

The element nitrogen (N), being a constituent of many biomolecules, including all proteins and nucleic acids, is essential to all living organisms. For many organisms, nitrogen represents the limiting nutrient for growth. Nitrogen can exist in a number of different oxidation states, with the interconversion between these states constituting what is typically referred to as the global biogeochemical nitrogen cycle (Figure 1). The reductive conversion of nitrate (NO_3^-) to N_2 (called denitrification), the oxidative conversion of ammonia (NH_3) to nitrate (called nitrification), and the interconversion between ammonia and organic forms of nitrogen (called assimilation and deamination) are catalyzed

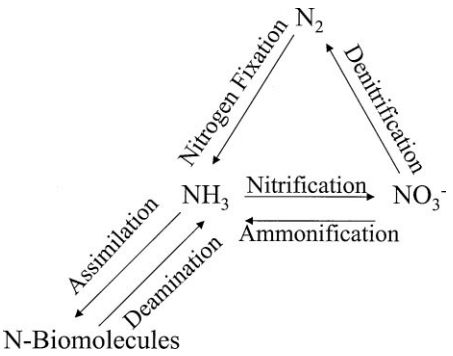

FIGURE 1. Global nitrogen cycle.

by an array of fascinating enzymes, many of which occur only in microorganisms and many of which contain unique and complex metal containing cofactors. More about these processes and the enzymes involved can be found in a number of excellent recent reviews (Arp, 2000; Ferguson, 1998; Finan *et al.*, 2002; Zumft, 1997).

N_2, constituting ~80% of air, represents the single largest reservoir of accessible nitrogen. Nitrogen oxides trapped in rocks and sediments probably represent a larger total quantity of nitrogen, but this nitrogen, for the most part, is not accessible to living organisms. The reductive conversion of N_2 into ammonia, called nitrogen fixation, occurs via a number of routes. Lightning strikes account for approximately 1% of the total N_2 fixed per year (total N_2 fixed $\sim 3 \times 10^{14}$ g/year). A major route for N_2 fixation is the industrial Haber–Bosch reaction used in nitrogenous fertilizer production (about 50% of the total N_2 fixed per year) (Finan *et al.*, 2002). This process, first described by Fritz Haber in 1908 (Haber, 1922; Haber & Le Rossignol, 1908) and later optimized by Carl Bosch, converts N_2 from air into ammonia using high pressures (200 atm.) of N_2 and H_2, high temperatures (450°C), and Fe based catalysts (Smil, 2001). Ammonia production via this process is a significant industrial endeavor, with the input of this fixed N into the biosphere having a profound impact on life, including human population growth (Smil, 2001). The other major route for N_2 reduction to ammonia occurs via biological nitrogen fixation (~50% of the total N_2 fixed per year). Biological nitrogen fixation is the exclusive domain of microbes (called diazotrophs), with nitrogen fixing bacteria found in many different genera. While these diazotrophs utilize a wide array of metabolic strategies, a common feature in all is the presence of the metalloenzyme nitrogenase, the enzyme responsible for the reduction of N_2 to ammonia.

Nitrogenases come in many different forms, with the most common categorization having four different families based on the type of metal cluster constituting the N_2 binding site (*i.e.*, the active site). One family of nitrogenases is represented by the recently discovered enzyme from *Streptomyces thermoautotrophicus* (Ribbe *et al.*, 1997). This nitrogenase contains two component proteins. One component, a CO-dehydrogenase, oxidizes CO to CO_2 and reduces O_2 to the superoxide anion radical ($O_2^{-\cdot}$). The second component is a manganese-dependent oxidoreductase that oxidizes $O_2^{-\cdot}$, providing electrons to the N_2 and reducing the MoFeS active site (Ribbe *et al.*, 1997). The other three families of nitrogenase share many similarities to each other, with a distinguishing feature being the metal content of the active site (including either Mo, V, or Fe only). These nitrogenases all include a smaller component protein called the Fe protein (or dinitrogenase reductase). This component contains a [4Fe-4S] cluster and acts as a MgATP-dependent electron delivering protein to the larger component protein, called dinitrogenase, which contains the active site metal cluster (Burgess & Lowe, 1996). The larger component protein, in addition to the active site metal cluster, also contains another metal cluster, called the P-cluster ([8Fe-7S]), which is involved as an electron transfer intermediate. The general N_2 reduction reaction catalyzed by these enzymes is typically presented as shown in Equation 1:

$$N_2 + 8\,e^- + 16\,ATP + 8\,H^+ \rightarrow 2\,NH_3 + 16\,ADP + 16\,Pi + H_2 \qquad [1]$$

These three families of nitrogenase are coded for by unique genes, with modest sequence identity between the proteins in each family (Eady, 1996). A distinguishing feature of the members in each family is the metal constitution of their active sites. The best studied family of nitrogenases contains an active site metal cluster with the composition [7Fe-9S-1Mo-X-homocitrate] that is called FeMo-cofactor. The "X" represents a newly identified constituent of the FeMo-cofactor (Einsle *et al.*, 2002) and is discussed in a later section. The other two families appear to have similar metal clusters at the active site, with the exception that the Mo is replaced by either V or Fe. These latter two families of nitrogenase are often referred to as the alternative nitrogenases. These enzymes have been the focus of several recent reviews (Eady, 1996; Rehder *et al.*, 1998; Ruttimann-Johnson *et al.*, 1998).

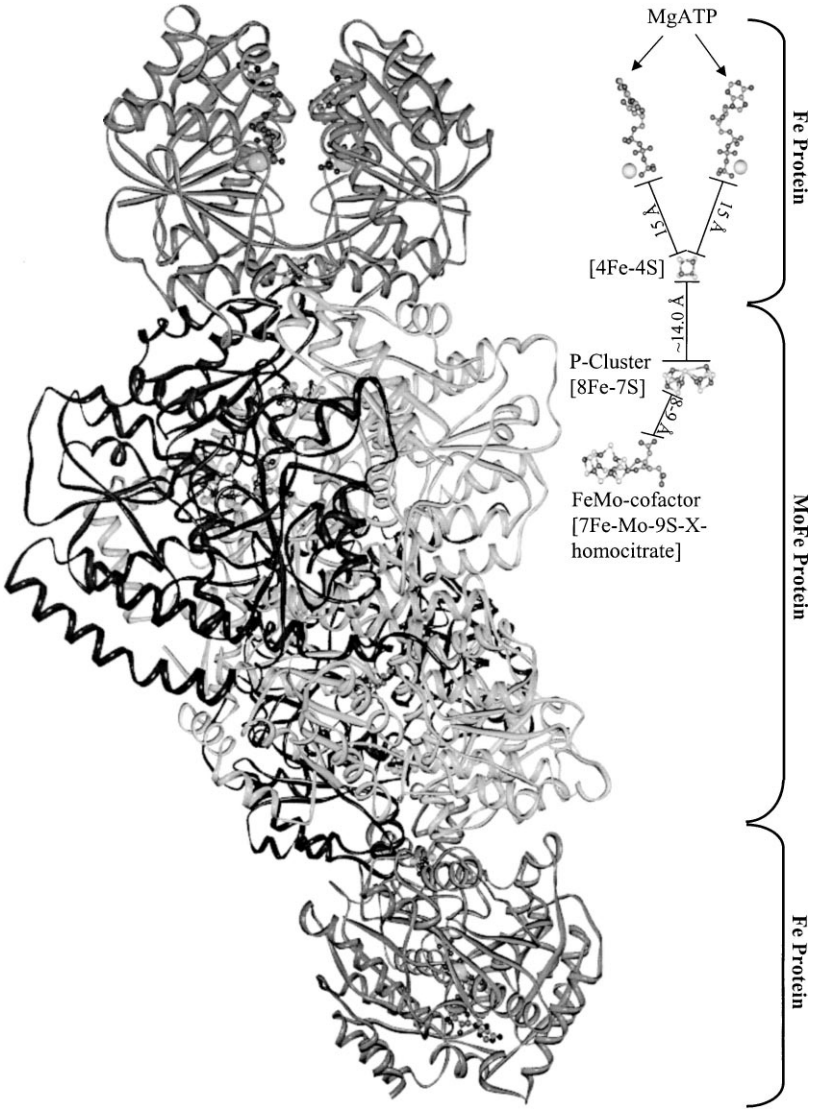

FIGURE 2. Overall structure of nitrogenase. Shown are α-carbon traces from the coordinates for the nitrogenase complex containing one MoFe protein (middle) and two Fe proteins (top and bottom) stabilized with the $\Delta 127^{Leu}$ Fe protein (PDB 1G21). The two α-subunits of the MoFe protein are colored the darkest, and the two β-subunits of the MoFe protein are colored the lightest. The two subunits of each Fe protein (top and bottom) are shown in intermediate gray. The relative positions of the bound MgATP molecules, the [4Fe-4S] cluster of the Fe protein, the P-cluster, and FeMo-cofactor of the MoFe protein for one-half of the nitrogenase complex are shown to the right.

This review focuses on the FeMo-cofactor containing nitrogenases, which are the paradigm for all other nitrogenases. The larger component protein of the Mo-dependent nitrogenase is called the MoFe protein (also called component I, or dinitrogenase) and is composed of two different polypeptides (coded for by the *nifD* and *nifK* genes) that are arranged as two dimers ($\alpha_2\beta_2$) (Figure 2). Each α-subunit binds a FeMo-cofactor, and the interface between each α-β dimer binds a P-cluster (an [8Fe-7S] cluster). The smaller component protein, called the Fe protein (also called component II, or dinitrogenase reductase), is coded for by the *nifH* gene, and is composed of two identical subunits (α_2) with a single [4Fe-4S] cluster bound between the subunits (Figure 2). The Fe protein also contains two MgATP binding sites, one on each subunit (Figure 2). There are other genes in the *nif* gene cluster that do not encode the nitrogenase component proteins but that do play roles in the maturation of nitrogenase and its

cofactors, or act as transcriptional regulators of the operon (Allen *et al.*, 1994; Dean & Jacobson, 1991; Schmitz *et al.*, 2002). The Mo-dependent nitrogenase has been isolated from a number of different organisms. Although the symbiotic *Rhizobia* are the most agriculturally important diazotrophic bacteria, the free-living soil bacteria are of great scientific importance for mechanistic studies because they are easily cultured. This review will focus on the Mo-dependent nitrogenase isolated from the free-living soil bacterium *Azotobacter vinelandii*, which has become the organism of choice for most nitrogenase studies.

In general terms, the consensus mechanism holds that the Fe protein with two bound MgATP molecules and its [4Fe-4S] cluster in the reduced (1+) oxidation state, binds to one half of the MoFe protein (an $\alpha\beta$-unit). This binding triggers the hydrolysis of the two MgATP molecules to two MgADP molecules already bound to the Fe protein, and the transfer of a single electron from the Fe protein into the MoFe protein (Figure 3). The initial recipient of the electron in the MoFe protein is presumed to be the P-cluster, which is thought to act as a mediator in electron transfer. Electrons (one or more) are then transferred to the FeMo-cofactor, where substrates bind and are reduced. After each intercomponent electron transfer event, the Fe protein must dissociate from the MoFe protein to be reduced by a small electron transfer protein (probably ferredoxin or flavodoxin) (Chatelet & Meyer, 2001; Hallenbeck & Gennaro, 1998)

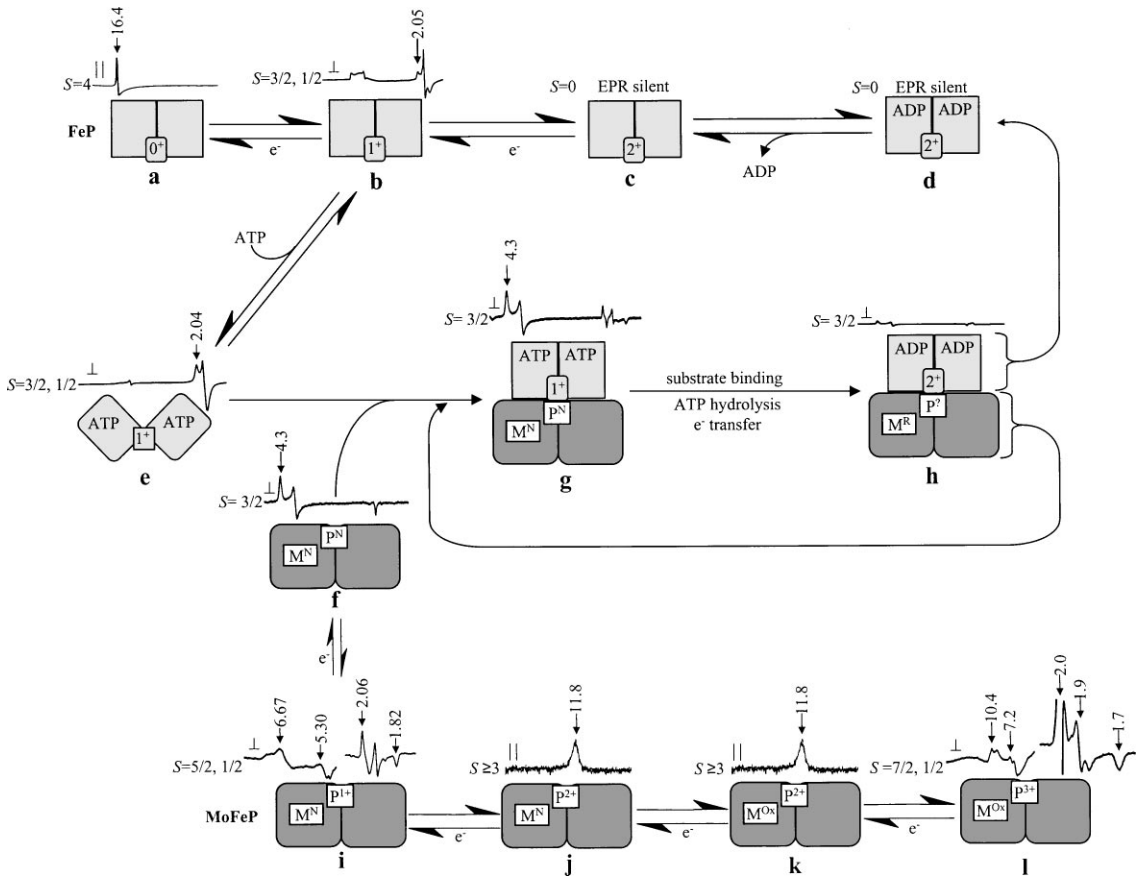

FIGURE 3. Schematic of the nitrogenase turnover cycle. One half of the MoFe protein (an $\alpha\beta$-unit) is shown as dark boxes (with the α-subunit to the left), while an Fe protein dimer is shown as lighter boxes. The [4Fe-4S] cluster of the Fe protein is shown as a smaller box within the Fe protein with the oxidation state noted. The P-cluster is shown as a smaller box in the MoFe protein at the $\alpha\beta$-subunit interface. FeMo-cofactor is shown as a smaller box in the α-subunit of the MoFe protein with an M in the middle. Representative EPR spectra are shown above each state of the protein components with arrows indicating typical *g*-values for the prominent inflections. The spin states for each are given along with perpendicular ($\perp$) and parallel ($||$) modes in the EPR.

and to exchange MgADP with MgATP. Thus, this cycle must be repeated at least 8 times for each equivalent of N_2 reduced and H_2 evolved.

A major advance in understanding the mechanism of the Mo-dependent nitrogenases came just over ten years ago with the solution of X-ray crystal structures for both the MoFe and Fe proteins from *A. vinelandii* (Bolin *et al.*, 1993; Chan *et al.*, 1993; Georgiadis *et al.*, 1992; Kim & Rees, 1992; Kim *et al.*, 1993). Since then, X-ray structures for several variants of these proteins have been presented (Jang *et al.*, 2000; Mayer *et al.*, 1999; Peters *et al.*, 1997; Sorlie *et al.*, 2001). The initial structures provided important observations, such as the disposition of subunits, the general location of the metal clusters, and models for the metal clusters. As with most significant advances, these structures posed an array of questions including:

How do substrates interact with the active site metal cluster, FeMo-cofactor, and what role does the protein play in defining reactivity?

How is the binding and hydrolysis of nucleotides on the Fe protein coupled to the rest of the nitrogenase mechanism?

How is electron transfer between the metal clusters controlled and what role do the P-clusters play?

As will be seen in this review, progress in recent years has been made on all of these questions, but for many, the core question remains. This review is organized following the general consensus mechanism (Figure 3), starting with the Fe protein and its binding of nucleotides, followed by the events occurring after the docking of the Fe protein with the MoFe protein, and ending with events occurring within the MoFe protein, culminating in the reduction of substrates, such as N_2 to ammonia.

II. IRON PROTEIN

The nitrogenase Fe protein is the only known reductant of the MoFe protein that will support substrate reduction. As noted earlier, the reduction of the MoFe protein by the Fe protein occurs during the transient association between these two proteins, and is coupled to the hydrolysis of MgATP on the Fe protein. Following these events, the Fe protein, now oxidized and with MgADP bound, dissociates from the MoFe protein to be reduced and to have MgADP exchanged with MgATP. Thus, the mechanism of the Fe protein can be seen to be composed of a cycle. This cycle, diagrammed in Figure 3 (Top), has been developed using a range of kinetic and spectroscopic methods. In the sections that follow, aspects of each step in the Fe protein catalytic cycle are reviewed.

A. Redox Properties of the Fe Protein

The [4Fe-4S] cluster of the Fe protein is bound between the two subunits, with 97^{Cys} and 132^{Cys} (*A. vinelandii* numbering) on each subunit providing the four protein ligands (Hausinger & Howard, 1982) (Figure 4). In the as-purified state, and in the presence of excess dithionite, the cluster is in a (+1) oxidation state with $3Fe^{2+}$ and $1Fe^{3+}$ (Hagen *et al.*, 1985a, 1985b; Lindahl *et al.*, 1985). In this oxidation state, the [4Fe-4S] cluster exhibits a mixed spin state $S = 1/2$ and $S = 3/2$ in the EPR (electron paramagnetic resonance) spectrum with g values near 2 ($S = 1/2$) and near $g = 4 - 3$ ($S = 3/2$) (Figure 3b) (Lindahl *et al.*, 1985). The relative proportions of the two spin states can be altered through the addition of various agents to the protein (*e.g.*, urea and glycerol) (Lindahl *et al.*, 1985). This indicates that solvent interaction may play a role in the properties of the [4Fe-4S] cluster.

The oxidized state of the Fe protein, with the [4Fe-4S] cluster in the 2+ oxidation state ($2Fe^{2+}$ and $2Fe^{3+}$), is achieved through oxidation by various agents, including O_2 (Thorneley & Ashby, 1989), redox active dye mediators (*e.g.*, methylene blue, indigo disulfonate, and thionine) (Watt & Reddy, 1994) (Figure 3b→c), and by electron transfer to the MoFe protein (Lindahl *et al.*, 1985) (Figure 3g→h). The oxidized (2+) state of the Fe protein is diamagnetic and thus EPR silent. The midpoint reduction potential (E_m) for the $[4Fe\text{-}4S]^{2+/1+}$ cluster couple has been determined by a range of voltametric and coulometric methods (Ryle *et al.*, 1995; Watt, 1979; Watt *et al.*, 1986). While values of E_m appear to depend on the organism from which the Fe protein is purified (Burgess & Lowe, 1996), values in the range of −300 mV are typical—this being the value measured for the Fe protein from *A. vinelandii* (Lanzilotta *et al.*, 1995b; Thorneley & Ashby, 1989; Zumft *et al.*, 1974).

The [4Fe-4S] cluster of the Fe protein can also be reduced to an all ferrous state (Figure 3b→a) with an overall oxidation state of (0) ($4Fe^{2+}$) (Angove *et al.*, 1997; Watt & Reddy, 1994). This is achieved by reduction with very low potential electron transfer agents such as Ti (III) citrate or reduced methyl viologen (Watt & Reddy, 1994). This reduced, or all

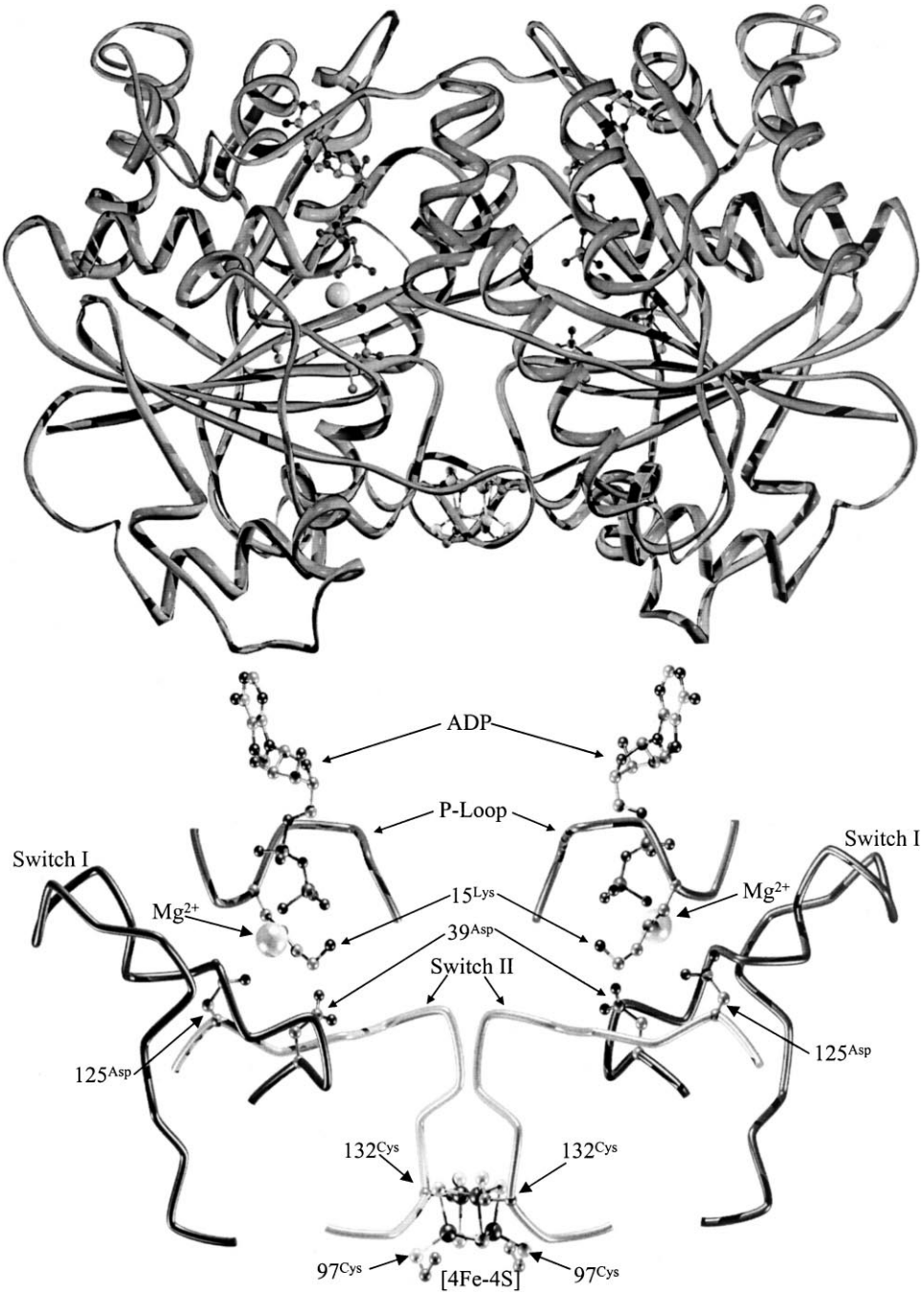

FIGURE 4. The Fe protein. A ribbon diagram for the Fe protein (top) taken from the coordinates (PDB 1FP6). The relative positions of MgADP, the [4Fe-4S] cluster, switch II, switch I, the P-loops, and the side chains of selected amino acids is also shown (below).

ferrous state, has been investigated using an array of spectroscopic methods (Musgrave *et al.*, 1998; Strop *et al.*, 2001; Yoo *et al.*, 1998), revealing that it is an integer spin state ($S = 4$) system with a parallel mode EPR signal at $g = 16.4$ (Figure 3a) (Angove *et al.*, 1998). The E_m for the $[4Fe\text{-}4S]^{1+/0+}$ cluster couple of the Fe protein has been the topic of some debate. The earlier value of -460 mV (Watt & Reddy, 1994) differs from the recently reported value of -790 mV (Guo *et al.*, 2002). Recent calculations using density functional theory (DFT) to estimate the E_m values for iron-sulfur clusters in various redox proteins (including the Fe protein) are most consistent with this more negative E_m (Torres

et al., 2003). The more negative value of −790 mV for the $[4Fe\text{-}4S]^{1+/0}$ couple would suggest that the all-ferrous state cannot be accessed *in vivo* since cellular reductants with sufficiently low E_m values are rare.

B. Nucleotide Binding to the Fe Protein

A requirement for MgATP in the nitrogenase reaction was recognized in the 1960s (Mortenson, 1964) and subsequent work has provided clear evidence that the Fe protein binds two equivalents of MgATP, one to each subunit (Mortenson *et al.*, 1993) (Figure 3b→e). Recent X-ray structures of the Fe protein with MgADP- or MgATP-bound have provided detailed views of the association between nucleotides and the Fe protein (Chiu *et al.*, 2001; Jang *et al.*, 2000; Schindelin *et al.*, 1997).

The affinity of Fe protein for binding nucleotides has been measured by several different techniques and a range of values for the dissociation constant (K_d) have been reported (Yates, 1991). This range of K_d values most likely reflects differences in affinity between proteins from different sources and differences in the methods used. Recently, isothermal titration calorimetry has been utilized to measure the affinity of binding nucleotides to the Fe protein. This method has the additional value of providing thermodynamic parameters ($\Delta G'^o$, $\Delta H'^o$, and $\Delta S'^o$) for the binding events (Lanzilotta *et al.*, 1999). These measurements have corroborated earlier conclusions that the Fe protein oxidized (2+) state binds MgATP with higher affinity (K_d = 45 μM) than does the reduced (1+) state (K_d = 500 μM). It was also concluded that the binding of the second MgATP molecule occurs with a higher affinity ($K_{d1} = 500\,\mu$M vs. $K_{d2} = 170\,\mu$M), thus supporting cooperative binding of nucleotides (Cordewener *et al.*, 1985). Like many nucleotide-utilizing enzymes, divalent metal ions are required for ATP binding. Mg^{2+} is likely to be the physiologically relevant metal for Fe protein, but other metals (*e.g.*, Mn^{2+}, Ca^{2+}, or Fe^{2+}) have also been shown to enable nucleotide binding (Weston *et al.*, 1983).

Early on it was recognized that the binding of nucleotides to the Fe protein caused changes in the properties of the protein, including the properties of the [4Fe-4S] cluster (Bui & Mortenson, 1968; Davis & Orme-Johnson, 1976; Mortenson *et al.*, 1973; Zumft *et al.*, 1974). Among changes in the [4Fe-4S] cluster are an increase in the accessibility of the Fe atoms to chelators such as α, α'-bipyridyl or bathophenanthrolinedisulfonate (Deits & Howard, 1989; Ljones & Burris, 1978; Walker & Mortenson, 1974). Other changes include alterations in the EPR spectrum and the E_m value. As discussed, the reduced [4Fe-4S] cluster of the Fe protein exhibits rhombic EPR signals from both $S = 1/2$ ($g = 2$ region) and $S = 3/2$ ($g = 5$) states (Figure 3b) (Lindahl *et al.*, 1985; Zumft *et al.*, 1973). These rhombic signals change lineshape, becoming more axial, when the Fe protein binds MgATP (Figure 3e) (Orme-Johnson *et al.*, 1972; Zumft *et al.*, 1973). The population of the $S = 3/2$ spin state relative to the $S = 1/2$ state decreases when the Fe protein binds MgATP (Orme-Johnson *et al.*, 1972; Zumft *et al.*, 1973). The binding of MgATP directly to the [4Fe-4S] cluster was ruled out early on (Morgan *et al.*, 1990), and the X-ray structures have revealed that MgATP binds some distance (∼15 Å) away from the [4Fe-4S] cluster (Chiu *et al.*, 2001; Georgiadis *et al.*, 1992; Jang *et al.*, 2000; Schindelin *et al.*, 1997).

Binding MgATP to the Fe protein also changes the E_m for the $[4Fe\text{-}4S]^{2+/1+}$ redox couple by −120 mV from −300 mV to −420 mV (Ryle *et al.*, 1996a; Thorneley & Ashby, 1989; Watt *et al.*, 1986; Zumft *et al.*, 1974). Binding MgADP to the Fe protein also decreases the E_m value by a comparable amount, but does not facilitate electron transfer (Moustafa & Mortenson, 1967). This change in the E_m value may be due to changes in the peptide environment of the [4Fe-4S] cluster as evidenced by changes in ^1H NMR spectra indicating that the environment of the cysteinyl (132^{Cys} and 97^{Cys}) α-CH and β-CH_2 protons change upon Fe protein binding MgATP (Lanzilotta *et al.*, 1995a; Meyer *et al.*, 1988). Although the above information suggests changes in the environment around the [4Fe-4S] cluster, there is evidence that little changes within the structure of the [4Fe-4S] cubane cluster itself upon MgATP binding. Studies using Fe-K edge X-ray absorption spectroscopy (Lindahl *et al.*, 1987; Ryle *et al.*, 1996b) indicate that the Fe-Fe or Fe-S bond distance does not change appreciably and neither do the frequencies of absorption bands in the resonance Raman spectrum upon nucleotide binding (Fu *et al.*, 1991; Ryle *et al.*, 1996b).

A central question has been how MgATP binding is communicated over 15 Å to alter the properties of the [4Fe-4S] cluster. It is clear that protein conformational changes must be the mechanism for this long-range communication. Large-scale conformational changes in the Fe protein upon binding nucleotides was confirmed by X-ray scattering studies that measured a decrease in the radius of

gyration of the Fe protein in the presence of MgATP (Chen *et al.*, 1994; Grossman *et al.*, 1997). The small decrease (R_g, = ~2 Å) is indicative of a slightly more compact structure in the Fe protein when MgATP is bound. While it is clear that the entire Fe protein changes conformation upon binding nucleotides, it is tempting to assume that specific segments of the Fe protein might play a more prominent role in the communication. A likely candidate for this role is the peptide section of the Fe protein leading from the MgATP binding site (125^{Asp}) to the [4Fe-4S] cluster ligand (132^{Cys}). This segment of the Fe protein is homologous to switch II found in other nucleotide binding proteins (*e.g.*, Ras P-21 and myosin) (Howard & Rees, 1994), which appears to function in communication from the nucleotide binding site across the protein (Figure 4). This short segment of peptide is thought to be a molecular switch to communicate the status of bound nucleotides to the [4Fe-4S] (Ryle & Seefeldt, 1996). A second peptide region in the Fe protein (amino acids 39–58) has been termed switch I, due to homology with a segment in other nucleotide binding proteins (*e.g.*, Ras P-21) (Figure 4) (Howard & Rees, 1994).

Prior to the elucidation of an X-ray structure of the Fe protein with nucleotides bound, Fe proteins with substituted amino acids (using site-directed mutagenesis) detailed the specific roles of many amino acids in various aspects of nucleotide interactions with the Fe protein. Substitution of 15^{Lys} and 125^{Asp} by other amino acids were found to produce Fe proteins that had altered behavior upon nucleotide binding. The $15^{Lys \rightarrow Gln}$ altered Fe protein was found to retain binding to MgATP, but the communication to the [4Fe-4S] cluster was disrupted (Ryle *et al.*, 1995). Substituting the 125^{Asp} to Glu was found to mimic some properties of the MgATP-bound form when MgADP was bound (Wolle *et al.*, 1992). The increased length of the carboxylate side chain with the Glu substitution probably forces interaction with the α- or β-phosphate of MgADP as it would occur to the β- or γ-phosphate of MgATP with the 125^{Asp} Fe protein. Also, in switch II, it was discovered that deletion of a Leu residue (127^{Leu}) forced the Fe protein into a conformation resembling an MgATP-bound state in the absence of any nucleotides (Ryle & Seefeldt, 1996). This $\Delta 127^{Leu}$ Fe protein variant does not hydrolyze nucleotides, but does dock to the MoFe protein to form a non-dissociating complex.

The availability of X-ray structures of Fe proteins with nucleotides bound have allowed a more detailed characterization of the nucleotide interaction site (Jang *et al.*, 2000; Rees *et al.*, 1998; Schindelin *et al.*, 1997). Comparison of the nucleotide-free Fe protein structure with that of the MgADP-bound Fe protein structure has identified a panoply of specific protein-nucleotide interactions, many of which manifest in changes in the position of the switch II polypeptide. MgADP exerts changes on switch II through a P-loop region that coordinates the Mg^{2+} by several carboxylates (*e.g.*, 39^{Asp}). Conformational changes of the P-loop (residues 11–16) are communicated through hydrogen bonding interaction of the peptide backbone amide of 14^{Gly} and then, in turn, to the hydrogen bonded carboxylate portion of 129^{Asp} which is part of switch II (Jang *et al.*, 2000). Movement of switch II results in changes in the position of the 132^{Cys} ligands of the [4Fe-4S] cluster (Chiu *et al.*, 2001; Schindelin *et al.*, 1997). Interestingly, the positions of the other set of cluster ligands (97^{Cys}) do not appear to change appreciably.

The combination of amino acid substitution studies and X-ray structures has yielded a fairly detailed view of the interactions between the Fe protein and nucleotides. Furthermore, specific segments of the Fe protein have been implicated in communication from the nucleotide binding site to the [4Fe-4S] cluster. Despite this progress, many of the details of correlating these structural changes and the known changes in the properties of the [4Fe-4S] cluster remain to be expounded upon.

C. Fe Protein-MoFe Protein Complex Formation

A series of events in the Fe protein catalytic cycle is initiated when the Fe protein docks with the MoFe protein (Figure 4e→g). Initial insights into the nature of the interaction between these two components came from examining the effects of salts on the protein-protein complex formation, and from the use of bifunctional cross-linking agents such as 1-ethyl-3-(3-dimethylaminopropyl)carbodiimide (Willing & Howard, 1990; Willing *et al.*, 1989). From these studies, specific residues on the Fe protein and MoFe protein involved in the docking interface were identified. These studies placed the docking surface on the Fe protein near the [4Fe-4S] cluster and on the MoFe protein near the α-β interface. More details on the docking interface have come from the examination of both Fe and MoFe proteins with amino acid substitutions in the putative interface (Christiansen *et al.*, 2000b, 2000c; Lowery *et al.*, 1989; Peters *et al.*, 1994; Seefeldt, 1994;

Wolle *et al.*, 1992). A significant advance in understanding the nature of the interactions between these two proteins has come from analysis of stable complexes formed between Fe and MoFe proteins. Several different stable tight complexes have been identified. The first was identified when Fe protein from *Clostridium pasteurianum* and the MoFe protein from *A. vinelandii* were mixed together (Emerich & Burris, 1976, 1978; Emerich *et al.*, 1978). A nondissociating complex was formed and characterized. Later, it was discovered that the addition of tetrafluoroaluminate (AlF_4^-), or beryllium fluoride (BeF_3^-) along with MgADP to functioning nitrogenase, inhibited the reduction of substrates and the hydrolysis of MgATP, resulting in the trapping of a stable Fe protein-MoFe protein nitrogenase complex (Clarke *et al.*, 1999; Duyvis *et al.*, 1996a; Miller *et al.*, 2001; Renner & Howard, 1996). The AlF_4^- was proposed to bind to the Fe protein in the same position as the γ-phosphate portion of MgATP. Subsequent determination of an X-ray structure of the Fe protein-MoFe protein complex trapped with AlF_4^- confirmed the presence of AlF_4^- (Schindelin *et al.*, 1997) where the γ-phosphate of MgATP would be expected. Importantly, this structure offered the first detailed view of the nature of the interactions between these two component proteins. A stable complex between the Fe protein where 127^{Leu} is deleted and the MoFe protein was also described (Lanzilotta *et al.*, 1997). A high resolution structure of this complex has recently been reported, including a structure with MgATP bound (Chiu *et al.*, 2001). The combination of these two structures of nitrogenase complexes has provided many details about the nature of the interactions between the two proteins. A comparison of the isolated nucleotide-free Fe protein structure to that of the MgATP-bound $\Delta 127^{Leu}$ Fe protein complexed to the MoFe protein shows that both switch I and switch II undergo significant movement (Figure 5). It is difficult to strictly ascribe the specific contributions to the observed conformational changes to nucleotide binding or complex formation. It is clear however, that the movement of switch I and II peptide segments have a role in defining the properties of the [4Fe-4S] cluster, binding to the MoFe protein, and triggering MgATP hydrolysis.

In addition to the structures, having stable Fe protein-MoFe protein complexes in hand has allowed many properties of the complex to be examined. For example, the E_m value for the metal clusters of the two nitrogenase proteins has been determined in the complex, with remarkable shifts in E_m values observed. The E_m of the Fe protein $[4Fe\text{-}4S]^{2+/1+}$ redox couple in the complex formed between the $\Delta 127^{Leu}$ Fe protein and MoFe protein was measured to be -620 mV (a shift of over -200 mV from the E_m when the protein is not in complex with the MoFe protein) (Lanzilotta & Seefeldt, 1997). Similarly, a -80 mV shift (from -300 to -380 mV) was observed for the E_m of the $P^{2+/N}$ redox couple of the P cluster (Table 1) (Lanzilotta & Seefeldt, 1997). Similar shifts in the E_m for the $[4Fe\text{-}4S]^{2+/1+}$ redox couple were observed in the nitrogenase complex

TABLE 1
Redox Potentials of Nitrogenase Metal Clusters

			E_m (mV)		
		Redox Couple	Isolated	In Complex	(References)
Fe Protein	No Nucleotides	$[4Fe\text{-}4S]^{1+/0}$	-790		(Guo *et al.*, 2002)
	No Nucleotides	$[4Fe\text{-}4S]^{2+/1+}$	-300		(Lanzilotta *et al.*, 1995b)
	With MgATP	$[4Fe\text{-}4S]^{2+/1+}$	-430	-620	(Lanzilotta *et al.*, 1995b; Lanzilotta & Seefeldt, 1997)
	With MgADP	$[4Fe\text{-}4S]^{2+/1+}$	-440		(Lanzilotta *et al.*, 1995b)
MoFe Protein	P-Cluster	$P^{1+/N}$	-300	-390	(Thorneley & Ashby, 1989)
		$P^{2+/1+}$	-300 (pH 8.0)*		(Lanzilotta & Seefeldt, 1997)
		$P^{3+/2+}$	$+90$		(Thorneley & Ashby, 1989)
	M-Cluster	$M^{N/(R\text{ or }I)}$**	~ -465		(Watt *et al.*, 1980)
		$M^{OX/N}$	-42		(Morgan *et al.*, 1988)

*$P^{2+/1+}$ redox couple is pH dependent (-53 mV/pH).
**$M^{N/(R\text{ or }I)}$ redox couple is an estimation based on controlled potential electrolysis (Watt *et al.*, 1980).

stabilized by MgADP-AlF_4, where the E_m was shifted from −300 mV to a value more negative than −500 mV (Spee *et al.*, 1998). The causes for the decrease in redox potential for the [4Fe-4S] cluster of the Fe protein are thought to be the effects of peptide conformational changes around the cluster and desolvation (Kurnikov *et al.*, 2001; Ryle *et al.*, 1996a). Both the [4Fe-4S] cluster and the P-cluster become better reductants within the Fe protein-MoFe protein complex, clearly favoring electron transfer through these clusters to the FeMo-cofactor active site.

D. MgATP Hydrolysis and Electron Transfer

Once the Fe protein has docked to the MoFe protein, MgATP hydrolysis in the Fe protein is activated and electron transfer from the Fe protein to the MoFe protein occurs (Figure 3g→h). The Fe protein alone does not catalyze MgATP hydrolysis at appreciable rates. Once bound to the MoFe protein in the proper conformation, however, the MgATP hydrolysis reaction is activated to rates of about ∼5000 nmoles MgATP hydrolyzed/min/mg of Fe protein. How the MoFe protein activates MgATP hydrolysis within the MoFe protein is curious given that the MoFe protein docks approximately 17 Å away from the nucleotide binding sites. This arrangement clearly points to some communication from the docking interface to the MgATP binding site. Clearly, protein conformational changes induced by component protein docking must be at play in activating MgATP hydrolysis. Given the prominent role of switches I and II within the Fe protein in nucleotide signal transduction, it seems reasonable that communication from the MoFe protein back into the Fe protein might use the same switches.

Within switch II, 129^{Asp} is in close proximity to the γ-phosphate of MgATP and has been implicated in playing a role in the hydrolysis reaction (Schindelin *et al.*, 1997). One model holds that upon Fe protein docking to the MoFe protein, communication through switch II repositions 129^{Asp} such that the carboxylate side chain could deprotonate a bound water molecule to form a hydroxide. The hydroxide then attacks the γ-phosphate of MgATP, initiating hydrolysis of the β-γ phosphodiester bond. The properties of Fe proteins with 129^{Asp} substituted by Glu are consistent with a role for this amino acid in hydrolytic events (Lanzilotta *et al.*, 1995b). Substitution of 129^{Asp} by Glu results in a Fe protein that still binds MgATP and docks to the MoFe protein, but does not hydrolyze MgATP to MgADP and Pi. A residue in a homologous position in other nucleotide dependent switch proteins has also been assigned a role as a general base, similar to the role just outlined for Asp^{129} of the Fe protein (Howard & Rees, 1994). Evaluation of the MgATP-bound state of the $\Delta 127^{Leu}$ Fe protein when complexed with the MoFe protein corroborates the critical role of the switch II region within the Fe protein. The deletion of 127^{Leu} causes the 129^{Asp} residue to be moved closer to a position that would promote MgATP hydrolysis (Chiu *et al.*, 2001).

Comparison of the structures of MgATP-bound $\Delta 127^{Leu}$ Fe protein in complex with the MoFe protein to the nucleotide-free Fe protein (Figure 5) suggests that switch I (residues 40–56) may also have a role as a trigger for nucleotide hydrolysis (Jang *et al.*, 2000). The switch I peptide segment that runs from the MoFe protein docking surface helices (residues 57–67) to 39^{Asp} may also experience conformational movement upon MoFe protein docking. Similar to the proposed function of Asp^{129}, Asp^{39} may participate by generating a nuclophilic hydroxide, which in turn is involved in hydrolysis. Substitution of Asp^{39} by Asn still allows the Fe protein to bind nucleotides and to dock to the MoFe protein (Lanzilotta *et al.*, 1997). Yet, the $39^{Asp→Asn}$ Fe protein does retain some MgATP hydrolysis activity, so 39^{Asp} cannot be the sole residue that acts in hydrolysis.

Since the Fe protein requires a trigger to activate MgATP hydrolysis, the obvious question is what on the MoFe protein activates this trigger? It has been shown that substitution of either of the two surface Phe residues on the MoFe protein (α–125^{Phe} or β–125^{Phe}) by Ala causes a decrease in proton reduction activity (Christiansen *et al.*, 2000b). When both of these residues are changed to Ala in the same MoFe protein, no electron transfer from the Fe protein to the MoFe protein and no MgATP hydrolysis is detected. It was proposed that these Phe residues could activate the triggers on the Fe protein, initiating MgATP hydrolysis (Christiansen *et al.*, 2000b).

While some MgATP utilizing enzymes form a phospho-enzyme intermediate (Andersen & Sorensen, 1996), this is not the case for the Fe protein (Mortenson *et al.*, 1985). This suggests that the energy released from the hydrolysis of the MgATP β-γ phosphodiester bond is directly channeled to peptide conformational changes that initiate other events such as electron transfer or dissociation of the component proteins.

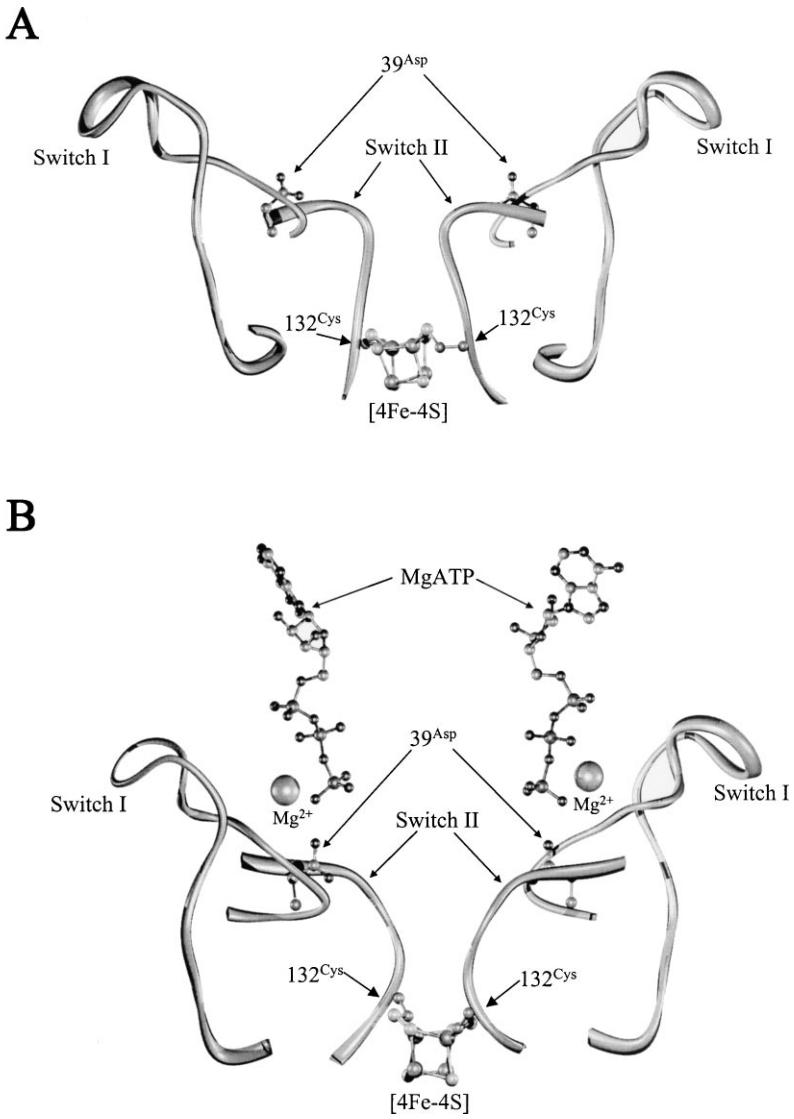

FIGURE 5. Conformational changes in the Fe protein upon docking to the MoFe protein. Portions of the Fe protein and [4Fe-4S] cluster are shown in the nucleotide-free state (Panel A) taken from PDB 1NIP and after $\Delta 127^{Leu}$ Fe protein docking to the MoFe protein and MgATP binding (Panel B) taken from PDB 1G21.

Electron transfer from the [4Fe-4S] cluster of the Fe protein to the MoFe protein (probably initially to the P-cluster as discussed below) appears to be intimately coupled to both the MgATP binding and hydrolysis events. The details of how MgATP binding or hydrolysis promotes the transfer of an electron remains one of the significant open questions in the nitrogenase mechanism. While these two events, MgATP hydrolysis and electron transfer, are linked, they are not obligatory. Both MgATP hydrolysis in the absence of electron transfer and electron transfer in the absence of MgATP hydrolysis have been demonstrated. Hydrolysis of MgATP can occur at significant rates (~500 nmoles/min/mg Fe protein) when the Fe protein is mixed with the MoFe protein without any source of electrons to support electron transfer (so called reductant independent ATP hydrolysis) (Cordewener *et al.*, 1988; Larsen *et al.*, 1995). The independence of the electron transfer event from MgATP hydrolysis has also been shown under special circumstances. The $\Delta 127^{Leu}$ Fe protein, which is altered in the switch II region and is found to mimic the MgATP-bound conformation, can transfer a single electron to the MoFe protein in the absence of MgATP binding or hydrolysis (Lanzilotta *et al.*, 1996).

Although the events of electron transfer to the MoFe protein and nucleotide hydrolysis within the Fe protein are not strictly required for the other reaction, it is clear that they influence each other. Rates of electron transfer from the Fe protein to the MoFe protein significantly accelerate when MgATP hydrolysis is functioning. Electron transfer occurs at a relatively low rate ($k = 0.007\ s^{-1}$) within the heterologous complex formed between the *C. pasteurianum* Fe protein and the *A. vinelandii* MoFe protein in the absence of MgATP. When MgATP is added, the rate increases by $\sim 10^4$-fold ($k \sim 100\ s^{-1}$) (Chan *et al.*, 1999b). This latter value is the rate constant measured for normally functioning nitrogenase.

From the above, it is clear that MgATP hydrolysis functions to accelerate electron transfer between the Fe protein and the MoFe protein. The details of how this occurs remain to be elucidated. A study of the temperature dependence on the rate of primary electron transfer from the Fe protein to the MoFe protein revealed that this electron transfer event is gated by some adiabatic process (Lanzilotta *et al.*, 1998b). It seems reasonable to conclude that this gating is related to MgATP hydrolysis.

How could MgATP hydrolysis influence the rate of electron transfer? It seems likely that this must occur through peptide conformational changes induced within the nitrogenase complex. In order to accelerate the rate of electron transfer, these peptide conformational changes must have the effect of either: a) increasing the difference in redox potentials of the redox pair (ΔE_m), b) decreasing the distance between the [4Fe-4S] cluster of the Fe protein and P-cluster of the MoFe protein, or c) altering the intervening medium or pathway to favor electron transfer, or some combination of the above (Davidson, 2000, 2002; Langen *et al.*, 1996; Sun & Davidson, 2002). The rate of electron transfer is clearly favored by a translation of the [4Fe-4S] cluster in the Fe protein $\sim$5 Å closer to the P-cluster when the Fe protein docks to the MoFe protein (Figure 5) (Chiu *et al.*, 2001; Schindelin *et al.*, 1997). Also favoring electron transfer in the Fe protein-MoFe protein complex is the increase in the ΔE_m (E_m Fe protein$^{2+/1+}$ – E_m P$^{OX/N}$) by over -150 mV (Lanzilotta & Seefeldt, 1997; Spee *et al.*, 1998). Both of these changes of electron transfer parameters will contribute to the rate of acceleration for electron transfer. Finally, inspection of the crystal structures of various nitrogenase complexes (Rees *et al.*, 1998), when combined with calculations (Kurnikov *et al.*, 2001), suggest one preferred electron transfer pathway from the Fe protein to the P-cluster in the MoFe (Figure 6). It is easy to imagine how MgATP-induced protein conformational changes could alter this electron transfer pathway, especially the through-space jumps, thus regulating electron transfer rates. It remains to be determined how MgATP hydrolysis changes this proposed pathway.

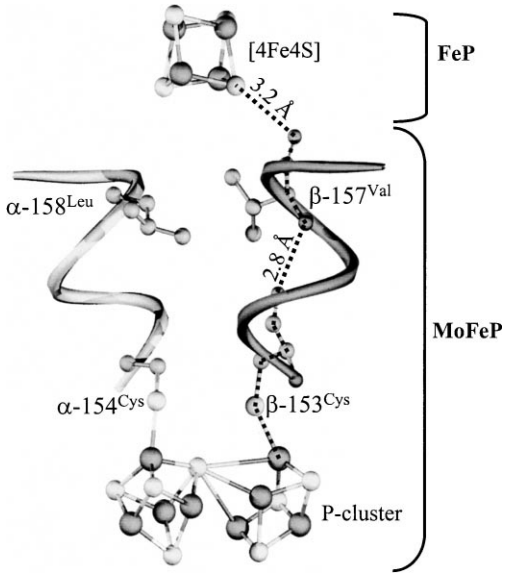

FIGURE 6. Putative electron transfer pathway from the [4Fe-4S] cluster to the P-cluster. A possible electron transfer pathway between the [4Fe-4S] cluster of the Fe protein and the P-cluster of the MoFe protein is shown. α-carbon traces for two α-helices in the α and β subunits of the MoFe protein are shown, along with the ligands to the P-cluster. The dashed lines highlight the putative electron transfer pathway calculated from the program HARLEM (Kurnikov *et al.*, 2001).

E. Dissociation of the Fe Protein from the MoFe Protein

Following MgATP hydrolysis and electron transfer from the Fe protein to the MoFe protein, the consensus model holds that the Fe protein dissociates from the MoFe protein (Figure 3h→d). (Hageman & Burris, 1978; Thorneley & Lowe, 1983). First order rate constants (k) have been reported for this step, with values between 2 to 6 s^{-1} depending on the source of the nitrogenase components (Duyvis *et al.*, 1998; Lowe & Thorneley, 1984a, 1984b). Based on computer simulations of

the overall kinetics of the nitrogenase reaction, this dissociation step has been proposed to be the rate-limiting step for catalysis (Thorneley & Lowe, 1985; Wilson *et al.*, 2001). It has been also suggested that when the Fe protein attains the MgADP-bound conformation at the end of its catalytic cycle, this is accompanied by a decreased affinity for the MoFe protein, thereby initiating complex dissociation. A related suggestion is that the energy released from the hydrolysis of MgATP directly promotes the dissociation of the complex (Cordewener *et al.*, 1987; Kurnikov *et al.*, 2001). The strongest support for these views comes from two cases where the Fe protein is arrested in a state prior to achieving the MgADP conformation. Inclusion of AlF_4^- during nitrogenase turnover arrests the enzyme in a state prior to the MgADP state. In this case, the Fe protein makes a non-dissociating complex with the MoFe protein (Duyvis *et al.*, 1996a; Renner & Howard, 1996). Likewise, the deletion of 127^{Leu} in switch II of the Fe protein locks the Fe protein into an MgATP-like state (Lanzilotta *et al.*, 1996). Again, the inability to achieve the MgADP-bound conformation results in the formation of a non-dissociating complex with the MoFe protein.

An alternative model suggests that the Fe protein does not need to dissociate from the MoFe protein during catalysis (Duyvis *et al.*, 1996b). In support of this model is evidence that MgATP can exchange with bound MgADP in some non-dissociating Fe protein-MoFe protein complexes (Lanzilotta *et al.*, 1996). There is also evidence from kinetic studies suggesting that at least several rounds of electron transfer can occur from the Fe protein before it dissociates from the MoFe protein (Duyvis *et al.*, 1997).

Contrary to the above model, a number of studies point to the need for the Fe protein to dissociate from the MoFe protein following each round of electron transfer. For example, the earlier kinetic studies indicated that the Fe protein must dissociate following each electron transfer event (Hageman & Burris, 1978). There is also the observation that the $\Delta 127^{Leu}$ Fe protein, when complexed to the MoFe protein, can transfer a single electron to the MoFe protein, but not subsequent rounds of electron transfer (Lanzilotta *et al.*, 1996). This in spite of the fact that the Fe protein [4Fe-4S] cluster can be reduced while still in the complex by flavodoxin or other mediators. This result clearly points to a need for dissociation of the component proteins as a prerequisite to each electron transfer event.

III. MOLYBDENUM-IRON PROTEIN

The MoFe protein component of nitrogenase contains the active site metal cluster, FeMo-cofactor, and the [8Fe-7S] (or P-) cluster. As noted earlier, the $\alpha_2\beta_2$ MoFe protein can be thought of as two catalytic $\alpha\beta$-units, with each $\alpha\beta$-unit containing one P-cluster and one FeMo-cofactor. There appears to be some communication between the $\alpha\beta$-dimeric units of the MoFe tetramer, where events on one $\alpha\beta$-dimer can have remote effects on properties of the other $\alpha\beta$-dimer (Clarke *et al.*, 2000; Maritano *et al.*, 2001). From the recent structures of Fe protein-MoFe protein complexes, it is clear that the Fe protein associates at the interface between an $\alpha\beta$-unit of the MoFe protein (Figure 2). Just below this docking surface lies the P-cluster. This arrangement strongly suggests that the P-cluster accepts electrons transferred from the Fe protein, although a definitive demonstration of the exact role of the P-cluster remains to be presented. Approximately 15 Å further away from the P-cluster, located entirely within the α-subunit of the MoFe protein, resides the FeMo-cofactor. The general picture that emerges regarding the mechanism of nitrogenase is Fe protein docking on the MoFe protein near the P-cluster, transfer of an electron to the P-cluster, followed by transfer of one or more electrons from the P-cluster to FeMo-cofactor, where substrates are reduced. This section of the review is organized following the electrons to the P-cluster, and finally, to the FeMo-cofactor. As will be seen, while significant progress has been made in understanding some of the details of events in the MoFe protein, many aspects of this portion of the mechanism remain unresolved.

A. P-Cluster Structure and Oxidation States

While the X-ray structure of the MoFe protein provided the structure for the P-cluster, and clearly suggested a role as the immediate electron acceptor from the Fe protein, details about the P-cluster have been slow to unravel. Prior to the initial determination of the structure of the P-cluster by X-ray crystallography (Chan *et al.*, 1993; Kim & Rees, 1992), the structure of the P-cluster was actively speculated based on information from several spectroscopic studies. Early Mössbauer spectroscopy of the MoFe protein oxidized to different degrees with thionine had revealed the total number of iron atoms (Zimmermann *et al.*, 1978). It was proposed that the

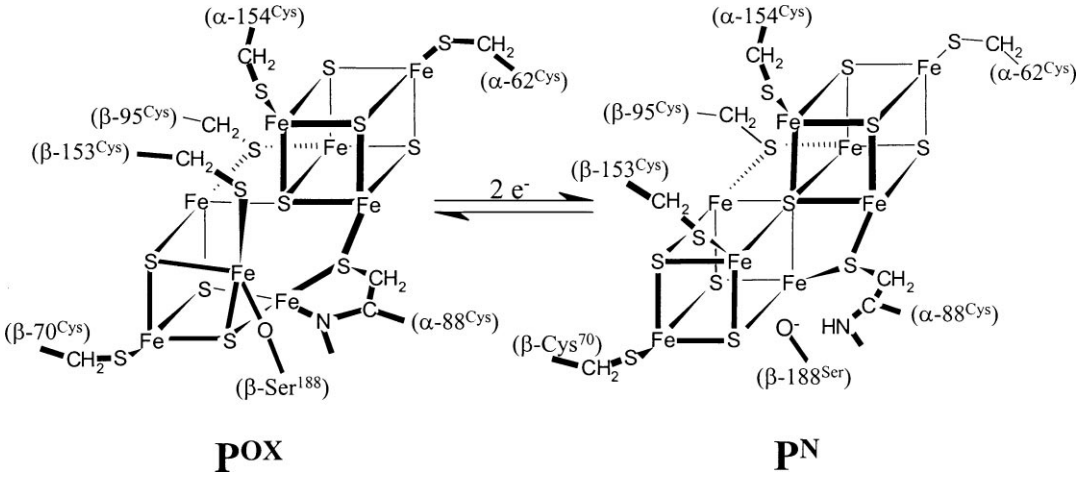

FIGURE 7. Oxidation states of the P-cluster. Schematic showing the P-cluster in the reduced P^N (right) and two electron oxidized P^{2+} (also called P^{ox}, left) oxidation states taken from the coordinates (PDB 2M1N and PDB 3M1N) (Peters *et al.*, 1997).

P-cluster was biologically unique and composed of two typical [4Fe-4S] clusters where a single Fe atom has a high-spin ferrous character. It was later proposed that the P-cluster was composed of a single [8Fe-7S] cluster based on EPR spectroscopy analysis of MoFe protein oxidized with solid thionine where new signals were observed at $g = 10.4$, 5.8 and 5.5 (Hagen *et al.*, 1987). These signals were ascribed to a partially oxidized P-cluster with a mixed spin state of $S = 7/2$ and $S = 1/2$ and allowed for the conclusion that each $\alpha\beta$–dimer of the MoFe protein contained one P-cluster (Pierik *et al.*, 1993).

Details of the P-cluster structure were elucidated by a series of X-ray structures of the MoFe protein (Chan *et al.*, 1993; Kim & Rees, 1992; Peters *et al.*, 1997). These structures revealed that the P-cluster was a unique [8Fe-7S] metal cluster composed of two [4Fe-4S] cubanes that shared a single μ_6-sulfide in the middle (Figure 7). Two thiolates from β-95^{Cys} and α-88^{Cys} also form bridges between the two iron-sulfur cubanes. Several earlier studies had indicated that the P-cluster could undergo multiple redox changes (Equation 2). When the MoFe protein is isolated with excess dithionite, the P-cluster is in the P^N state where all of the Fe atoms are essentially ferrous (Zimmermann *et al.*, 1978). From the P^N state, the P-cluster can be oxidized to several more states using oxidative dyes such as thionine or indigo carmine (Lindahl *et al.*, 1988; Pierik *et al.*, 1993; Surerus *et al.*, 1992; Tittsworth & Hales, 1993). Each of these more oxidized states have unique paramagnetic spectroscopic signatures.

$$P^{Red} \underset{}{\overset{E_{m0} = ?\ mV}{\rightleftharpoons}} P^{N} \overset{E_{m1} = -309\ mV}{\rightleftharpoons} P^{1+} \overset{E_{m2} = -309\ mV}{\rightleftharpoons} P^{2+} \overset{E_{m3} = +90\ mV}{\rightleftharpoons} P^{3+} \quad [2]$$

The one electron oxidized P^{1+} state is a mixed spin state with $S = 1/2$ and $S = 5/2$ and gives rise to perpendicular mode EPR signals at $g = 2$ ($S = 1/2$) and at $g = 5$–8 ($S = 5/2$) (Figure 3i) (Tittsworth & Hales, 1993). The P^{2+} state has a parallel mode EPR signal at $g = 11.8$ that is due to an integer spin $S \geq 3$, non-Kramers system (Figure 3j) (Pierik *et al.*, 1993). One proposed model of the P-cluster being oxidized to the P^{1+} state is that each half of the P-cluster can be independently oxidized with the observed mixed population of $S = 5/2$ and $S = 1/2$ spin states (Tittsworth & Hales, 1993). Upon oxidation of both halves of the P-cluster to the P^{2+} state, spin coupling can occur giving rise to the parallel mode EPR signal at $g = 11.8$. This model is supported by similar E_m values for both the $P^{1+/N}$ and $P^{2+/1+}$ couples (-310 mV at pH 8.0), indicating that the first and second oxidation of the P-cluster occurs with similar overall thermodynamic difficulty (Tittsworth & Hales, 1993). Further oxidation to the P^{3+} (which is essentially irreversible) state can be achieved with solid thionine or by controlled O_2 exposure (Hagen *et al.*, 1987). The P^{3+} state is composed of a mixture of $S = 7/2$ and $S = 1/2$ spin states. EPR signals for the P^{3+} state can be observed at $g = 6$ and 11 for the $S = 7/2$ spin state and as a rhombic signal centered about $g = 1.9$

for the $S = 1/2$ spin state (Figure 3l) (Hagen *et al.*, 1987; Lindahl *et al.*, 1988).

B. Catalytic Role for the P-Cluster

As noted earlier, the consensus model states that the P-cluster accepts electrons from the Fe protein and donates electrons to FeMo-cofactor. Although this view is appealing, there is limited evidence to demonstrate this role for the P-cluster. For example, the oxidation state of the P-cluster that accepts electrons from the Fe protein remains unidentified. One of two scenarios seems likely. Either the P^N state is reduced by one or more electrons to an as yet undetected reduced state (P^R), or the P^N state is first oxidized (by sending electrons to FeMo-cofactor), with this oxidized state accepting electrons from the Fe protein. Regardless of which of these two scenarios is operative, it is clear that the intermediate state must be fleeting, since it has not been clearly detected. Very rapidly after an electron is transferred from the Fe protein into the MoFe protein, the FeMo-cofactor is reduced, supporting the observation that any involvement of the P-cluster must be transient (Smith *et al.*, 1973).

Two unusual properties of the P-cluster have emerged from recent studies, namely the observation of major structural changes upon oxidation or reduction and a pH dependence on the E_m value for one of the couples. Both of these observations point to unique features that may be operative during catalysis.

X-ray crystal structures of the MoFe protein in either an oxidized or a reduced state were compared (Peters *et al.*, 1997), revealing major structural differences between the states. In the reduced state (P^N), the central sulfur atom that bridges the two iron-sulfur cubanes has μ_6 ligation. Upon oxidation to the P^{2+} state (also called P^{OX}), this central μ_6S detaches from two of the irons and converts to a distorted tetrahedral arrangement (Figure 7). Also upon oxidation from the P^N to P^{2+} state, the P-cluster gains an Oγ ligand from β-188^{Ser} and an additional coordination from the peptide backbone amide of α-88^{Cys} (Figure 7) (Peters *et al.*, 1997). One of the suggestions from these structures was that such structural changes might be accompanied by protonation/deprotanation reactions, which in turn might make one or more of the E_m values for the couples dependent on pH. To explore this possibility, the E_m values for the $P^{2+/1+}$ and $P^{1+/N}$ redox couples were determined at various pH values. The E_m for the $P^{2+/1+}$ couple was indeed observed to vary with changing pH. The $P^{2+/1+}$ couple E_m was observed to change linearly over a pH range from 6.0 to 8.4 at -53 mV/pH unit (Lanzilotta *et al.*, 1998a). Alteration of pH was not found to have an effect on the E_m for the $P^{1+/N}$ couple. Therefore, the redox change from the P^{1+} to the P^{2+} state must involve the release of a proton, suggesting the P-cluster may have a role in coupled proton and electron transfer. Such coupling of proton and electron transfer have been observed in other Fe-S clusters, such as the [4Fe-4S] cluster found in *A. vinelandii* ferredoxin (Hirst *et al.*, 1998).

Site-directed mutagenesis studies have been employed in an effort to identify the source of the pH dependence on the E_m of the $P^{2+/1+}$ couple. The β-$188^{Ser\rightarrow Cys}$ altered MoFe protein was found to exhibit a novel EPR signal in the $g = 2$ region for the dithionite reduced state (Chan *et al.*, 1999a). The E_m of the $P^{2+/N}$ couple for this altered protein was found to be more negative (-480 mV, pH 8.0) and still pH dependent. Since the pH dependence on the $P^{2+/1+}$ couple E_m was retained in the β-$188^{Ser\rightarrow Cys}$ altered MoFe protein, the β-188^{Ser} hydroxyl group was concluded not to play a role in the redox coupled protonation. Interestingly, the resting state EPR spectrum in the β-$188^{Ser\rightarrow Cys}$ MoFe protein was observed to disappear during turnover with the Fe protein and MgATP, clearly pointing to the fact that the P-cluster changes redox states during nitrogenase turnover. This is probably the most direct evidence for a redox role of the P-cluster in catalysis, although the direction of change (*i.e.*, reduced or oxidized) was not clear.

Another study that points to a redox role of the P-cluster during nitrogenase catalysis involved a MoFe protein with the FeMo-cluster without *R*-homocitrate (Ma *et al.*, 1996). This protein was made *in vitro* by reconstituting the apo-MoFe protein isolated from a $\Delta nifH$ strain of *A. vinelandii* (Gavini *et al.*, 1994) with only the metal cluster portion of the FeMo-cofactor. The authors denoted this reconstituted MoFe protein, lacking the *R*-homocitrate moiety, as the MoFe-cluster containing MoFe protein. This MoFe-cluster containing MoFe protein was found to be EPR silent in the dithionite reduced state. Upon addition of Fe protein and MgATP to this altered MoFe protein, a new axial EPR signal in the $g = 2$ region was observed and was attributed to redox changes of the P-cluster. Removal of the homocitrate portion of the FeMo-cofactor may have stabilized a previously unobserved state of the P-cluster.

Two recent studies have also examined a form of the MoFe protein that is missing FeMo-cofactor (called apo-MoFe protein) (Christiansen *et al.*, 1998; Ribbe *et al.*, 2002). The apo-MoFe protein was isolated from either a Δ*nifB* or a Δ*nifH* strain of *A. vinelandii.* Deletion of either of these genes disrupts the biosynthesis of FeMo-cofactor. The apo-MoFe protein from the Δ*nifB* strain is EPR silent in the dithionite reduced state, but does elicit the parallel mode $g = 11.8$ signal upon oxidizing the P-cluster to the P^{2+} state. It was shown that the P^{2+} state of the P-cluster can be reduced to the P^{1+} state using Fe protein and MgATP (Christiansen *et al.*, 1998). This also supports the view that the P-cluster is involved in e^- transfer to the FeMo-cofactor. The Δ*nif*H apo-MoFe protein exhibits a strong $S = 1/2$ EPR signal in the $g \sim 2$ region in the dithionite reduced state, but does not show the $g = 11.8$ signal characteristic of a normal P^{2+} state. This Δ*nif*H apo-MoFe protein does facilitate MgATP hydrolysis when associating with the Fe protein, but does not receive electrons from the $[4Fe\text{-}4S]^{1+}$ cluster of the Fe protein (Ribbe *et al.*, 2002). This altered P-cluster was able to be reduced using the stronger reductant Ti(III) citrate, but the unusual spectroscopic properties suggest the presence of a P-cluster precursor.

Assuming that the P-cluster does act as an electron transfer intermediate, then electrons must be passed to the FeMo-cofactor. An absence of methods to isolate or to study changes in the MoFe protein during electron transfer from the P-cluster to FeMo-cofactor has made this secondary electron transfer event difficult to study. As in all biological electron transfer events, the overall efficiency of transfer is controlled by the distance between the P-cluster and FeMo-cofactor, the difference in the E_m values of the donor and acceptor (ΔE_m), and the nature of the intervening medium for electron transfer (Davidson, 2000; Dutton, 1996; Gray & Winkler, 1996). There is limited or no information about the E_m values that are operative in this electron transfer event. While we have E_m values for the $P^{2+/N}$ couple, there is not compelling evidence that this couple is relevant to catalysis. Likewise, we have no measured values for the E_m for the reduction of FeMo-cofactor ($M^{N/R}$ couple). There is also limited information about the possible changes in distance between the P-cluster and FeMo-cofactor during catalysis. More information can be gleaned about possible electron transfer pathways by examining the structures of the MoFe protein. Four parallel α-helices located between the P-cluster and FeMo-cofactor can be identified (Chan *et al.*, 1993). Two of these helices are initiated with

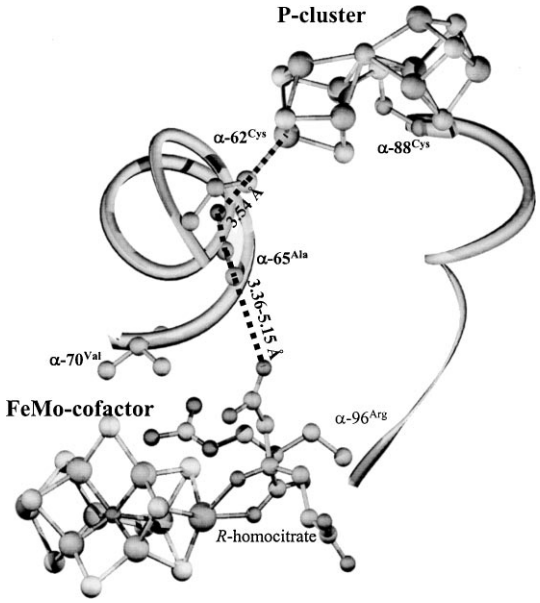

FIGURE 8. Putative electron transfer pathway from the P-cluster to FeMo-cofactor. A possible electron transfer pathway from the P-cluster to FeMo-cofactor is shown. α-carbon traces for portions of the α-subunit are shown as ribbons. The electron transfer pathway calculated using the program HARLEM is shown as a dashed line (PDB 1G21). The distance between the β-methyl carbon of α-65^{Ala} to the *R*-homocitrate carboxylate is shown as a range, because the distance varies depending on the structure used.

ligands to the P-cluster (α-88^{Cys} and α-62^{Cys}) and lead to residues near FeMo-cofactor (α-96^{Arg} and α-70^{Val}) (Figure 8). These helices may provide a medium for electron transfer from the P-cluster to the FeMo-cofactor. To examine this possibility, we have recently performed pathway calculations using the computer program HARLEM (Figure 8). A number of different calculations using several different structures of MoFe proteins all identified a single favored pathway for electron transfer (dashed line in Figure 8). The pathway starts with an electron exiting the P-cluster through the α-62^{Cys} thiol ligand, traveling a short distance through the helix to the methyl side chain of α-65^{Ala}, and then entering the FeMo-cofactor through homocitrate, on the Mo end of FeMo-cofactor. This pathway involves two through space jumps, which have the most disruptive effect on the electron transfer pathway. Experiments are needed to test this possible electron transfer pathway.

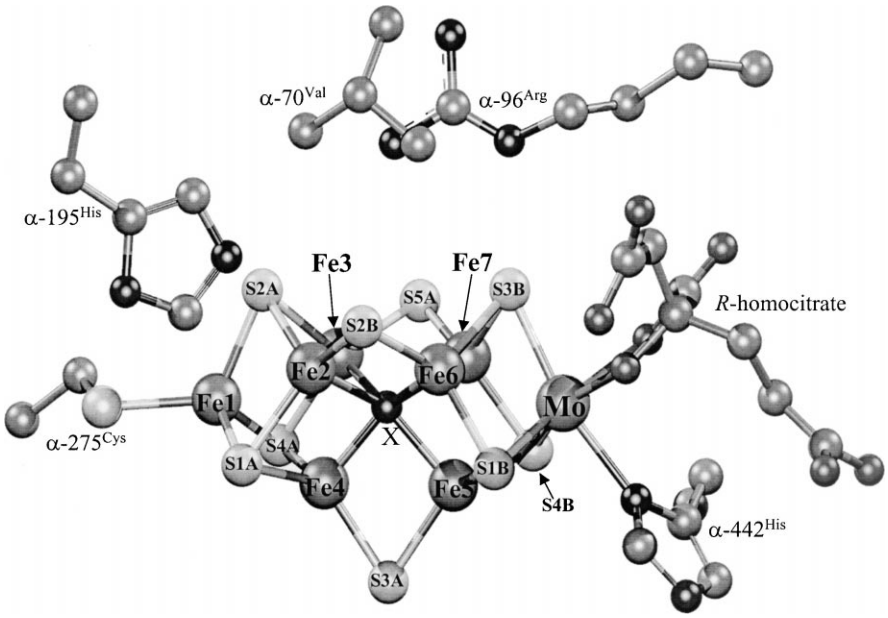

FIGURE 9. FeMo-cofactor. Structure of the FeMo-cofactor with some amino acids of the MoFe protein (PDB 1M1N). The numbering of the Fe and S atoms is as described earlier (Einsle *et al.*, 2002).

Clearly, the topic of the role of the P-cluster in electron transfer, and the pathway of transfer to FeMo-cofactor remains largely uncharted territory in the nitrogenase mechanism.

C. FeMo-Cofactor Structure and Oxidation States

The determination of the structure of the MoFe protein in 1992 provided the first view of the structure of the active site FeMo-cofactor (Kim & Rees, 1992). Subsequent studies have refined aspects of this structure, leading to the current model of this cofactor being a [7Fe-9S-Mo-X-homocitrate] cluster (Figure 9) (Chan *et al.*, 1993; Einsle *et al.*, 2002; Mayer *et al.*, 1999). The overall cluster is composed of two subclusters that are bridged by three μ_2-sulfides. One subcluster is typical of a [4Fe-4S] cluster, while the other subcluster is essentially a [4Fe-4S] cubane with molybdenum replacing one of the Fe atoms at the terminal end of the cluster. Homocitrate is bound through two oxo-ligands of the C1 carboxylate and C3 hydroxylate to the Mo. An atom, denoted as X, has recently been identified in the center of FeMo-cofactor in a very high resolution X-ray structure of the MoFe protein (1.16 Å) (Einsle *et al.*, 2002). The identity of this atom is currently unknown, but heavy metals have been ruled out based on diffraction properties. The density is most consistent with X being N, C or O. One of the interesting aspects of the original structure of FeMo-cofactor (*i.e.*, before X was in the middle) was the presence of 6 Fe atoms at the waist of the cluster with trigonal coordination. The addition of X would suggest that some or all of these Fe atoms may be tetrahedral rather than trigonal.

It is worth noting that while the metal cluster portion of FeMo-cofactor has c3 symmetry, the *R*-homocitrate ligand and protein environment of the MoFe protein where FeMo-cofactor is bound is not symmetrical. The molybdenum is ligated by the δN of α-442^{His}, along with the two oxo ligands provided by homocitrate, thus giving the molybdenum a pseudo-octahedral coordination. On the other terminal end of the FeMo-cofactor, the terminal Fe is ligated by the thiolate of α-275^{Cys}.

The observation of an atom X in the middle of FeMo-cofactor has prompted debate on its identity and its potential role in catalysis. One suggestion has been that if X is nitrogen, then it could be exchangeable during reduction of N_2. This model has been tested recently by allowing nitrogenase to turnover in the presence of $^{15}N_2$, followed by analysis of the protein by ENDOR (electron nuclear double resonance) and ESEEM (electron spin echo envelope modulation) spectroscopies (Lee *et al.*, 2003). The conclusion from these studies is that if X is N, it is not exchangeable during catalysis. The identity of X is not clarified in this study. Computational methods

have also been applied toward resolving the identity of the central ligand X of the FeMo-cofactor (Dance, 2003; Hinnemann & Norskov, 2003). These studies conclude that X being N would be more energetically favorable than other soft atoms.

Not surprising for such a complex metal cluster, FeMo-cofactor can undergo a number redox reactions (Equation 3).

$$M^{Ox} \underset{}{\overset{E_{m1} = -40\ mV}{\rightleftharpoons}} M^{N} \overset{E_{m2} = -465\ mV}{\rightleftharpoons} M^{R} \quad [3]$$

The resting state of the MoFe protein, isolated in the presence of the reductant dithionite, has FeMo-cofactor in the M^N state. In this state, FeMo-cofactor is paramagnetic with an $S = 3/2$ spin state with a well characterized axial EPR spectrum with inflections at $g = 4.3$, 3.7 and 2.0 (Figure 3f) (Orme-Johnson *et al.*, 1972). This EPR spectrum has been a vital tool in studying the nitrogenase catalytic cycle, providing a spectroscopic fingerprint. The M^N state of the FeMo-cofactor can be reversibly oxidized by one electron to a state called M^{OX} (Figure 3k) using a variety of mediator dyes (*e.g.*, thionine) (Lindahl *et al.*, 1988; Zimmermann *et al.*, 1978). The M^{OX} state is diamagnetic ($S = 0$) and therefore is EPR silent. An E_m of about -40 mV (Table 1) has been measured for the $M^{OX/N}$ couple using controlled potential coulometry (Schultz *et al.*, 1988) and other techniques (O'Donnell & Smith, 1978).

When Fe protein, MgATP, and a reductant (*e.g.*, dithionite) are added to the MoFe protein, substrate reduction begins. If suitable substrates are not present, then protons are reduced to make H_2. If the MoFe protein is trapped during this steady-state turnover condition, the FeMo-cofactor is observed to be predominantly in a state more reduced than the M^N state (Huynh *et al.*, 1980; Yoo *et al.*, 2000). This more reduced state is designated as M^R. It is worth noting that the M^R state may in fact represent a number of different states of FeMo-cofactor. The M^R state is diamagnetic, and has been determined to be an integer spin ($S \geq 1$) state that is EPR silent (Huynh *et al.*, 1980). The E_m for the $M^{N/R}$ couple has never been directly measured, although the value has been estimated to be < -465 mV (Watt *et al.*, 1980).

Characterization of the M^R state by Mössbauer spectroscopy revealed few differences from the M^N state, where the average isomer shift (δ_{av}) only changed by 0.002 mm/s. This suggested that the seven Fe sites experience only small changes in electron density and have the same spin structure. It was postulated that if the addition of an electron(s) does not significantly alter the electronic properties of the Fe sites, then the reduction must be associated with the Mo atom (Yoo *et al.*, 2000). An alternative reduced state of the MoFe protein was produced by irradiating the protein using synchrotron radiation. Mössbauer analysis of this radiolytically reduced sample (called M^I) showed significantly different electronic character about the Fe sites, clearly indicating differences from the M^R state (Yoo *et al.*, 2000). The M^R state has also been examined using both Fe and Mo-edge EXAFS (extended X-ray absorption fine structure) spectroscopy (Christiansen *et al.*, 1995). The M^R state for that study was created using a low Fe protein to MoFe protein ratio, which allows for a slow turnover and significant population of the M^R state. This EXAFS study inspected the M^{OX}, M^N, and M^R states. The Fe-Fe bond distances were found to be successively shorter as the FeMo-cofactor was reduced. The shortening of the Fe-Fe bond distances also suggested that the central cavity of FeMo-cofactor becomes larger as the FeMo-cofactor becomes more reduced.

The oxidation states of the Fe atoms in the resting state of FeMo-cofactor have been vigorously debated. Mössbauer spectroscopy using MoFe protein with FeMo-cofactor selectively enriched with ^{57}Fe has suggested valence assignments of [$1Mo^{4+}$, $3Fe^{3+}$, $4Fe^{2+}$, $9S^{2-}$] (Yoo *et al.*, 2000). In contrast, ENDOR studies have suggested a valence assignment of [Mo^{4+}, $1Fe^{3+}$, $6Fe^{2+}$, $9S^{2-}$] (Lee *et al.*, 1997b). A computational study using density functional theory (DFT) was most consistent with a valence assignment of [Mo^{4+}, $1Fe^{3+}$, $6Fe^{2+}$, $9S^{2-}$], in agreement with the ENDOR studies (Lovell *et al.*, 2001). However, these calculations utilized a FeMo-cofactor structure not having X at the middle. Interestingly, new calculations on FeMo-cofactor with X in the middle has led to a different preferred valence assignment of [$1Mo^{4+}$, $3Fe^{3+}$, $4Fe^{2+}$, $9S^{2-}$], now consistent with the Mössbauer study (Lovell *et al.*, 2003).

FeMo-cofactor can be extracted from the protein using the organic solvent N-methylformamide (NMF), and numerous studies have been performed on this isolated cofactor as a way to gain insights into its properties. When isolated in organic solvent, the cofactor is typically referred to as the FeMo-cluster. A recent electrochemical analysis of FeMo-cluster has examined the redox interconversions that are analogous to the M^{OX}, M^N, and M^R states (Pickett *et al.*, 2003). The detailed cyclic voltammetry experiments performed in this study

show that isomerization of the solvent ligands can affect the electrochemical properties of the FeMo-cluster. The same study included Fourier Transform Infrared (FTIR) spectroelectrochemistry to investigate how CO binding affects the cluster, and concluded that the CO bound state used in the ENDOR studies may be comparable to the two e^- reduced state. Therefore, the valence assignment of [$1Mo^{4+}$, $3Fe^{3+}$, $4Fe^{2+}$, $9S^{2-}$] from the Mössbauer spectroscopy (Yoo *et al.*, 2000) may be appropriate for the M^N state and the valence assignment from ENDOR analysis (Lee *et al.*, 1997b) is suitable for a more reduced CO bound state. The isomerization of ligands to the FeMo cluster that is shown in this study also indicates that conformational movement of FeMo-cofactor ligands (α-275^{Cys}, α-442^{His} and *R*-homocitrate) may have significant effects on the electrochemical properties of the active site metal cluster.

D. Interactions of Substrates and Inhibitors at the Active Site

One of the more intense areas of nitrogenase research in the last several years has focused on the identification of the exact binding site and binding modes of substrates and inhibitors on FeMo-cofactor, and the role of the surrounding protein in regulating FeMo-cofactor reactivity. These endeavors have utilized four main methods: 1) site-directed mutagenesis to change amino acids in the MoFe protein, 2) use of a range of substrates and inhibitors as probes of the active site, 3) trapping nitrogenase during turnover by rapid freezing or chemical quenching, and 4) use of a host of advanced spectroscopic methods to detect and characterize species bound to FeMo-cofactor. These approaches, applied individually or in combination, have provided considerable insights into the key questions about the active site. However, as will be apparent, this area of nitrogenase research is still lacking significant information.

Essential to progress in understanding the nitrogenase mechanism has been the utilization of a range of substrates and inhibitors. Generally, nitrogenase substrates are small, uncharged and have olefinic bonds. Some of the most noteworthy substrates are: N_2, H^+, N_2H_4, N_3^-, $CH_3C{\equiv}CH$, $C_2H_5C{\equiv}CH$, $H_2C{=}C{=}CH_2$, methyl isocyanide, cyanide, cyanamide, acetylene, ethylene, N_2O, and CS_2. Previous reviews have discussed the reactivity of nitrogenase towards these compounds and the respective products (Burgess, 1985; Burgess & Lowe, 1996). Utilization of several of these compounds to understand nitrogenase binding of substrates is highlighted in the following sections.

Carbon monoxide (CO) is a potent inhibitor of all nitrogenase substrate reduction reactions except for proton reduction (Hardy *et al.*, 1965). Early on, it was discovered that trapping nitrogenase under turnover conditions in the presence of CO results in changes to the FeMo-cofactor EPR spectrum. The $S = 3/2$ spectrum of FeMo-cofactor changed to an $S = 1/2$ spin state upon addition of low concentrations of CO (0.08 atm of CO) giving rise to a new EPR signal (denoted lo-CO) with $g = 2.09, 1.97, 1.93$. At higher concentrations of CO (0.5 atm), a different EPR signal is observed (called hi-CO) with inflections at $g = 2.17, 206, 2.06$ (Davis *et al.*, 1979; Hwang *et al.*, 1973). These early observations suggested that there were multiple binding sites on the FeMo-cofactor for CO. ^{13}C-ENDOR spectroscopy studies by Hoffman, Hales, and coworkers using ^{13}C-enriched CO confirmed that two CO molecules are bound to the FeMo-cofactor under hi-CO conditions (Pollock *et al.*, 1995). It has also been demonstrated that these bound CO molecules are labile and readily exchangeable (Cameron & Hales, 1998; Maskos & Hales, 2003). An ENDOR study using ^{57}Fe incorporated into the MoFe protein showed that CO was bound to one or more Fe atoms in the FeMo-cofactor. More detailed analysis by orientation selective ^{13}C and ^{1}H Q-band ENDOR spectroscopy yielded information on the sites of CO binding and possible protonation events associated with CO binding. This analysis showed that CO is bound in a bridging mode across two iron atoms for the lo-CO state and two CO molecules bind to two separate iron atoms in the hi-CO state (Lee *et al.*, 1997a).

Carbon disulfide (CS_2) can be reduced by nitrogenase to H_2S and some unidentified CS species. The slow turnover rate for reduction of this substrate allowed three intermediates to be trapped by rapid freeze quench. These intermediates were detected as new EPR signals (Ryle *et al.*, 2000). ^{13}C-ENDOR analysis of this freeze-trapped intermediate made with ^{13}C-labeled CS_2 established that these novel CS_2-derived EPR signals all resulted from CS_2 reduction intermediates that are bound to the FeMo-cofactor. An analysis of the temporal development of these EPR signals revealed a sequential formation over 1 min. The first intermediate formed was postulated to have trigonal ligation of a C and one S to one or more Fe atoms. The two species that developed next were suggested to be bound end on with C to an Fe atom.

It has been abundantly clear for many years that the MoFe protein greatly influences the reactivity of FeMo-cofactor. This is most evident from the fact that FeMo-cofactor isolated away from the protein into organic solvents does not have the same reactivity as FeMo-cofactor in the protein (Smith, 1999; Smith *et al.*, 1999). Therefore, changing amino acids within the MoFe protein that might influence FeMo-cofactor reactivity has been an area of intense research. Of some interest has been a recent series of studies using site-directed mutagenesis, coupled with use of alternative substrates, freeze-quench methods, and spectroscopic methods that appear to have localized substrate binding sites on FeMo-cofactor. These studies started with a genetic approach aimed at illuminating areas of FeMo-cofactor where substrates bind (Christiansen *et al.*, 2000a). In short, mutant strains of *A. vinelandii* were created that discriminated between acetylene and nitrogen as substrates for nitrogenase. Normally, nitrogen reduction activity of nitrogenase is inhibited by acetylene in a noncompetitive fashion where acetylene consumes the reductive equivalents (Dilworth, 1966; Hwang *et al.*, 1973; Rivera-Ortiz, 1975). Therefore, diazotrophic growth of *A. vinelandii* can be inhibited when the cells are cultured under acetylene. A series of random mutants in the MoFe protein were created, and the cells expressing these altered MoFe proteins were challenged to grow diazotrophically under a partial atmosphere of acetylene gas (Christiansen *et al.*, 2000a). A number of acetylene resistant colonies were isolated, and genetic analysis mapped to the same amino acid substitution, a substitution of α-69^{Gly} by Ser in the α-subunit of the MoFe protein. Subsequent analysis of the purified α-$69^{Gly\rightarrow Ser}$ MoFe protein verified that this amino acid substitution greatly decreases the affinity for binding acetylene, without altering the affinity for binding N_2. Furthermore, acetylene became a competitive inhibitor of N_2 reduction, clearly pointing to a common binding site. Amino acid α-69 is adjacent to α-70^{Val}, which is part of the first sphere of residues surrounding the FeMo-cofactor. The Val side chain of α-70 is directly above a 4Fe face of FeMo-cofactor consisting of Fe2, Fe3, Fe7, and Fe6 (numbering of Fe atoms taken from PDB file 1M1N) (Figure 9). This study clearly pointed to this face of FeMo-cofactor as being a possible site for substrate binding.

This initial study was followed up by several subsequent studies that have focused on the amino acids near this face. In one such study, it was discovered that larger substrates could be accommodated into the nitrogenase active site by shortening the side chain of α-70^{Val} (Mayer *et al.*, 2002). For example, changing α-70^{Val} to Ala greatly increases the reduction activity for propyne and propargyl alcohol (HO─CH_3─C≡CH) (Mayer *et al.*, 2002). These three alkynes are normally very poor substrates for nitrogenase, and only become reasonable substrates when α-70^{Val} is changed to Ala or Gly. This observation further points to the FeS face composed of Fe2, Fe3, Fe7, and Fe6 as providing the site for substrate binding.

Another study has focused on α-96^{Arg}, located on this same face (Figure 9). The guanidinium portion of the side chain of α-96^{Arg} is proposed to be within hydrogen bonding distance (3.3 Å) to S5A. Changing this cationic guanidinium group by substituing with a series of other amino acids created MoFe proteins that allowed the detection of binding of the substrate acetylene or the inhibitor cyanide when the protein is in the resting state (Benton *et al.*, 2001b). Prior to this study, interactions of substrates or inhibitors with FeMo-cofactor were only observed when nitrogenase was trapped under turn-over conditions (requiring the Fe protein, MgATP, and an electron source), implying the need for turnover induced changes at or near FeMo-cofactor to allow substrate binding. Removal of the Arg side chain in the α-96 position appears to mimic the turnover-dependent changes near FeMo-cofactor. Q-band Mims ^{13}C-pulsed ENDOR spectroscopy of the α-96^{Leu} MoFe protein with ^{13}C-cyanide showed that the cyanide is bound to FeMo-cofactor, and the hyperfine coupling constants are consistent with binding to one or more Fe atoms.

In close proximity to α-70^{Val} and α-96^{Arg} near this 4Fe face of FeMo-cofactor is α-195^{His} (Figure 9). A series of earlier studies on MoFe protein with this residue changed to Gln or Asn all pointed to significant changes in the reactivity of FeMo-cofactor (Fisher *et al.*, 2000a, 2000b, 2000c; Kim *et al.*, 1995). Recently, it has been reported that an α-195^{Gln} MoFe protein could be trapped under turnover conditions with acetylene, yielding novel EPR signals arising from bound acetylene reduction intermediates (Sorlie *et al.*, 1999). By studying the power and temperature dependence of the new signals, it was possible to deconvolve the EPR spectrum into three different signals consisting of a rhombic signal ($g = 2.12, 1.98, 195$), an isotropic signal ($g = 2.0$), and a third signal ($g = 1.97$). Based on their electronic properties, the respective signals were assigned to an unpaired electron on the metal cluster for the rhombic signal and a carbon

radical for the isotropic signal. The radical nature of these species suggests that reduction of substrates (at least acetylene) may occur by a stepwise radical mechanism.

In summary, the application of alternative substrates, site directed mutagenesis to change amino acids, and spectroscopy have provided significant new information about substrate interactions with FeMo-cofactor. Despite this progress, there is clearly significant work to be done in order to provide a molecular level map of the nitrogenase mechanism.

E. Mechanism of Substrate Binding and Reduction

As noted earlier, the reduction of dinitrogen and other substrates by the MoFe protein requires two or more rounds of the Fe protein cycle (*i.e.*, Fe protein docking, MgATP hydrolysis, electron transfer, and Fe protein dissociation). Reactions such as proton (Equation 4) or acetylene (Equation 5) reduction

$$2H^+ + 2e^- \rightarrow H_2 \qquad [4]$$

$$C_2H_2 + 2H^+ + 2e^- \rightarrow C_2H_4 \qquad [5]$$

require an accumulation of two electron equivalents in the MoFe protein, whereas reduction of other substrates requires from 2 to 8 electron equivalents (*i.e.*, dinitrogen reduction requires eight electron equivalents). It is apparent that the MoFe protein must be able to accumulate electrons for these different reactions. Where and how these electrons are accumulated is not exactly known. Some possible sites of accumulation include the P-cluster, FeMo-cofactor, bound hydrides, and partially reduced bound substrate intermediates (Burgess & Lowe, 1996; Dance, 1996; Thorneley & Lowe, 1984a). Making no assumptions about the location of the accumulated electrons, a model was developed that accounts for successive rounds of reduction of the MoFe protein by Lowe & Thorneley in the 1980's (Lowe & Thorneley, 1984a; Thorneley & Lowe, 1984a, 1984b, 1985). Their model was originally based on pre-steady state kinetics of the *Klebsiella pneumoniae* nitrogenase using stopped-flow spectrophotometry and rapid quench-EPR to detect intermediates such as diazine and hydrazine during nitrogen reduction. This model remains the best overall description of the nitrogenase mechanism. The Thorneley–Lowe cycle starts with the MoFe protein in its dithionite reduced state (E_0) and is followed by eight successive rounds of reduction to give further reduced states of the MoFe protein (E_1, E_2, E_3, ... E_7) (Figure 10). Each successive reduction of the MoFe protein requires one round of the Fe protein cycle and electron transfer into the MoFe protein.

Although reduction of dinitrogen requires only six electrons, eight cycles of the Fe protein (at minimum) are required due to the stoichiometric reduction of two protons that is observed when reducing N_2. Attempts to eliminate this obligate hydrogen evolution have been made by turning over the nitrogenase complex in excess of 50 atm of N_2, but the formation of hydrogen was persistently observed at a ratio of 1 H_2 formed for 1 N_2 reduced (Simpson & Burris, 1984). Due to this requirement of proton reduction, it is generally thought that proton reduction to yield H_2 is an intrinsic part of the

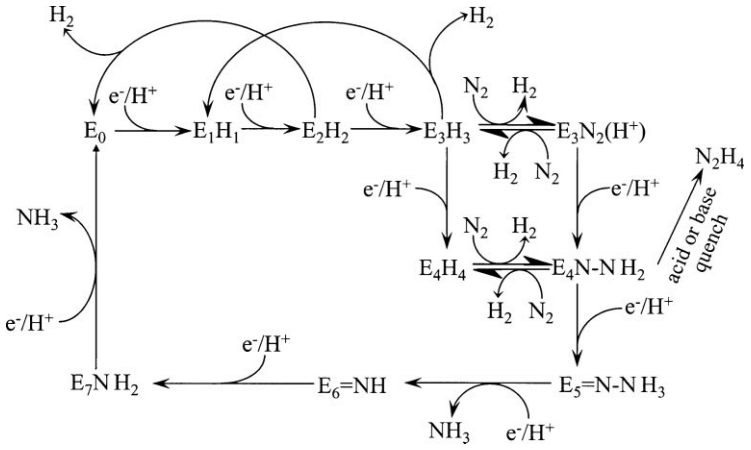

FIGURE 10. Modified Thorneley–Lowe kinetic scheme for the reduction of N_2. Adapted from (Thorneley & Lowe, 1985).

mechanism for N_2 reduction (Hadfield & Bulen, 1969; Rivera-Ortiz, 1975).

One of the key observations about the nitrogenase mechanism that is illustrated in the Thorneley–Lowe model is the fact that different substrates bind to different reduced states of the MoFe protein. A lag time is observed from the initiation of the nitrogenase turnover and the first detection of N_2 reduction intermediates such as diazine (N_2H_2) (Thorneley *et al.*, 1978) and hydrazine (N_2H_4) (Thorneley & Lowe, 1984a). This lag time has been interpreted to indicate that N_2 does not bind to the MoFe protein until a more reduced state is achieved (Figure 10). An important consequence of different substrates binding to different reduction states of the MoFe protein is that substrates that bind to more oxidized states can appear to be noncompetitive inhibitors of substrates that bind at more reduced states. This causes a phenomenon where substrates may appear to be non-competitive while binding to the same site.

Study of several site-specifically altered MoFe proteins have contributed to the development of a substrate reduction mechanism. One of the more extensively studied altered MoFe proteins is the α-$195^{His\rightarrow Gln}$ variant (Fisher *et al.*, 2000a, 2000b, 2000c; Kim *et al.*, 1995). Inspection of crystal structures of the MoFe protein reveal that the imidazole residue of α-195^{His} is also in close proximity to the previously discussed 4Fe face and also is within hydrogen bonding distance (3.3 Å) to one of the μ_2 sulfur atoms (S2B) associated with that 4Fe face (Figure 9). Replacement of this imidazole by an amide as in the α-$195^{His\rightarrow Gln}$ variant MoFe protein makes it incapable of dinitrogen reduction. Yet, it has been shown that this protein still binds N_2 by the fact that N_2 still can competitively inhibit reduction of acetylene and protons (Kim *et al.*, 1995). It has been proposed that the α-195^{His} residue is required to correctly position or protonate an N_2 reduction intermediate subsequent to initial binding.

As mentioned previously, proton reduction appears to be an intrinsic part of the N_2 reduction mechanism. In the absence of any other substrates, protons are reduced at a very efficient rate (2200 $nmol \cdot min^{-1} \cdot mg^{-1}$). One of the most peculiar aspects of dinitrogen reduction catalyzed by nitrogenase is the formation of HD when N_2 reduction proceeds under an atmosphere of D_2 gas. The observation that H_2 gas can inhibit HD formation has led to the hypothesis that dinitrogen binds the FeMo-cofactor by displacing a bound dihyrdride, thus giving the obligatory 1:1 stoichiometry of H_2 formed per reduced N_2 (Guth & Burris, 1983; Hughes *et al.*, 1989). The $\alpha 195^{His\rightarrow Gln}$ altered protein, which cannot reduce N_2, also catalyzes HD formation in the presence of N_2, further supporting the dihydride displacement upon N_2 binding (Fisher *et al.*, 2000c).

The stereospecificity of the hydrogenation of acetylene has provided some insights into the mechanism of substrate reduction. The reduction of C_2H_2 in D_2O by nitrogenase almost exclusively forms *cis*-$C_2H_2D_2$ (Dilworth, 1966). This observation has been used to support models of side-on binding mechanisms for acetylene at the FeMo-cofactor (Hardy *et al.*, 1968; Kelly, 1969). Two recent studies have investigated the effects of changing amino acid residues around the active site on the *cis*/*trans* ratio of acetylene hydrogenation. Newton and coworkers have examined the *cis*- and *trans*- ratio of acetylene reduction with the α-$191^{Gln\rightarrow Lys}$, α-$195^{His\rightarrow Gln}$, and α-$195^{His\rightarrow Asn}$ altered MoFe proteins (Fisher *et al.*, 2000a). The α-$191^{Gln\rightarrow Lys}$ and α-$195^{His\rightarrow Gln}$ MoFe proteins were found to form the *trans*-$C_2D_2H_2$ at a higher ratio (5-9-fold increase) compared to the wild-type MoFe protein (Fisher *et al.*, 2000a). A correlation was made between the increased fraction of *trans*-$C_2D_2H_2$ and the ability of these altered MoFe proteins to form ethane from ethylene. Recently, another study has inspected the tendency for other altered MoFe proteins to form the *trans*-$C_2D_2H_2$ isomer upon reduction of acetylene (Benton *et al.*, 2001a). MoFe protein variants altered at α-96^{Arg} and α-69^{Gly} were found to form significant amounts of the *trans*-$C_2D_2H_2$, and it was further found that the proportion of *trans*-isomer formed increased upon decreasing the overall electron flux into the MoFe protein (regulated by Fe protein: MoFe protein ratio) (Benton *et al.*, 2001a). To explain the formation of the *trans*-isomer, a mechanism of a branched reaction path with a bound η_2-vinyl intermediate was presented.

Understanding the role of *R*-homocitrate in FeMo-cofactor has remained a challenge. A role in both electron transfer from the P-cluster and as a proton donor seems reasonable. In a series of elegant studies, Ludden and coworkers synthesized several homocitrate analogs and incorporated them into FeMo-cofactor in the MoFe protein (Madden *et al.*, 1990, 1991). They observed that carboxylate groups at C1 and C2 and the hydroxyl group on C2 of the homocitrate are all crucial to support reduction of N_2. Recently, Smith & Henderson have proposed that *R*-homocitrate is required for substrate reduction because it is able to form hydrogen bonds with the α-442^{His} ligand to the Mo of the FeMo-cofactor,

thereby tuning electronic properties of the FeMo-cofactor (Grönberg *et al.*, 1998).

Beyond the studies mentioned above, there has been a paucity of experimental evidence to elucidate the substrate binding mechanism. This is apparent from the fact that a fundamental question such as whether substrates bind to the Mo or to the Fe atoms remains uncertain. One approach that has provided insights into possible substrate binding and reduction mechanism has been theoretical studies. These studies have addressed such questions as the oxidation states of the metals in FeMo-cofactor and P-clusters (Lovell *et al.*, 2001; Mouesca *et al.*, 1994), possible modes of substrate binding (Rod *et al.*, 1999), and possible mechanisms for substrate reduction (Dance, 1996, 1997; Durrant, 2002a). Several studies have also focused on determining the most likely binding sites and modes of N_2 to Fe atoms of the FeMo-cofactor (Dance, 1996, 1997; Rod & Norskov, 2000; Siegbahn & Blomberg, 1999; Siegbahn *et al.*, 1998). The partiality for N_2 binding at one or more of the Fe atoms comes, in part, from the observation that the Mo atom of the FeMo-cofactor can be replaced with either V or Fe in the alternative nitrogenases, and from the spectroscopy studies with CO (Lee *et al.*, 1997a), acetylene (Benton *et al.*, 2001b), CS_2 (Ryle *et al.*, 2000) and cyanide (Benton *et al.*, 2001b) that all point to binding to Fe atom(s). From the calculations, it appears that nitrogen can have several different binding modes:

1. N_2 bound perpendicular or parallel to the length of the cofactor,
2. N_2 bound to two to four Fe atoms,
3. N_2 bound end-on or side-on, and
4. N_2 bound in the central cavity of the FeMo-cofactor (Dance, 1996, 1997).

Proton addition to the cluster has also been addressed and it has been suggested that the μ_2S atoms are feasible sites for protonation (Rod & Norskov, 2000).

Some studies have favored N_2 binding to the Mo atom of the FeMo-cofactor as proposed in the Chatt cycle (Pickett, 1996). Recently, an investigation of N_2 binding and reduction to a portion of FeMo-cofactor has been conducted by comparing DFT energies of various isomers at every step of N_2 reduction (Durrant, 2002a). These studies conclude that binding of N_2 to Mo instead of Fe is substantiated by more favorable energetics. The binding and reduction of N_2 is proposed to proceed as follows (Figure 11):

1. One of the homocitrate ligands dissociates from the pseudooctahedral Mo atom upon protonation and reduction of Mo (IV) to Mo (III) (Figure 11, steps B→D). This is aided by hydrogen bonding properties of α-442^{His}.
2. N_2 is then bound end-on to the Mo atom (Figure 11D).
3. Partial reduction of the bound N_2 to a diazenido (NNH) intermediate occurs next, resulting in a change in the ligation to a bridging fashion between the Mo and one Fe (Figure 11D→E).
4. Next, the diazenido is reduced to a diazene ligated to the Mo (Figure 11D→E).
5. The bound diazene is then converted to a linear hydrazido-bound species (Figure 11E→F).
6. Further reduction cleaves the N─N bond (Figure 11G→H).
7. The Fe bound amine is protonated, resulting in the formation of the first ammonia molecule (Figure 11H→I).
8. The reduction of the Mo bound nitride then occurs to yield the second ammonia (Figure 11H→I).

An important aspect of this model is that it fits with the Thorneley–Lowe cycle and it attempts to account for the effects of various site-specifically altered MoFe proteins. This study represents the most complete analysis reported to date of each step in the N_2reduction reaction. Durrant also addresses the mechanism for hydrogen evolution and H/D scrambling on a state of the FeMo-cofactor with bound dinitrogen (Durrant, 2002b). It is worth noting that all of these calculations were done on a portion of FeMo-cofactor that included 1Mo-1Fe-3S. How inclusion of the remainder of FeMo-cofactor (including X) will impact this model will be interesting.

Many theoretical studies have been performed to address the substrate reduction question in nitrogenase and have yielded a range of solutions. Clearly, there is a significant need for new experimental results to support one or more of these models before we can move to the next level in understanding the nitrogenase mechanism.

A final issue for consideration is how substrates (including protons) gain access to FeMo-cofactor from the surface of the MoFe protein and how reduction products exit. Durrant has recently identified a water filled channel that leads from the surface of the MoFe protein to a pool of water molecules located near homocitrate of FeMo-cofactor (Figure 12, bottom). He has proposed that this channel offers a way to shuttle protons to the active site, as well as provide

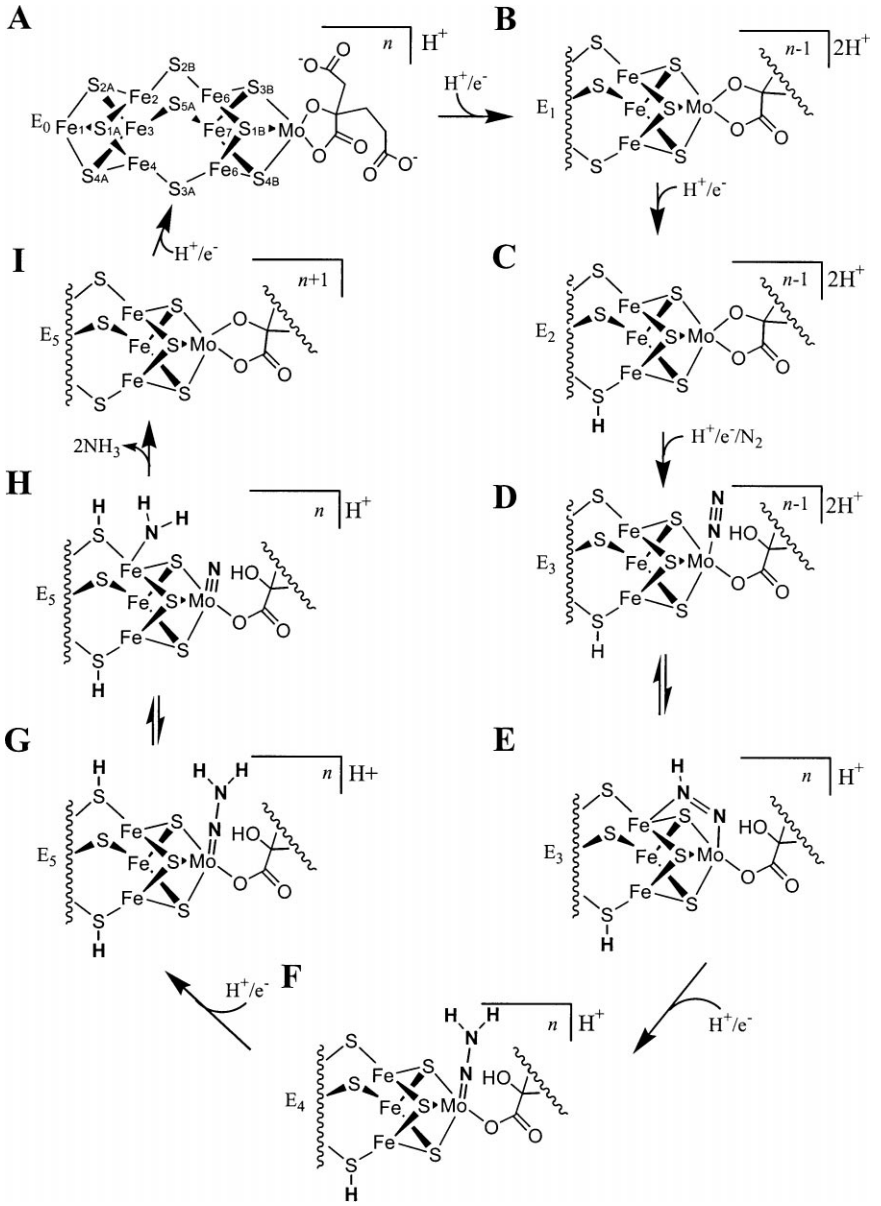

FIGURE 11. Proposed mechanism for N_2 reduction. Proposed mechanism for N_2 reduction on FeMo-cofactor based on theoretical calculations (Durrant, 2002a). The corresponding states from the Thorneley and Lowe model (E_0, E_1, etc.) are shown to the left of each state. The number (*e.g.*, n-1) within the bracket to the top right indicates the redox state relative to the resting M^N state. The number of protons shown to the right of the bracket represents protons not localized that may be associated with the protein or homocitrate. Adapted from (Durrant, 2002a).

a channel for gas (*e.g.*, N_2, acetylene, etc.) entry and product (*e.g.*, NH_4^+, ethylene, etc.) egress from FeMo-cofactor. He also highlights two additional channels that could provide a means for delivery of protons to the active site by utilizing a proton relay mechanism.

We have recently identified another possible channel that leads from the surface of the MoFe protein to FeMo-cofactor. This hydrophobic channel (Figure 12, top) has several attractive features that suggest that this may be the mechanism for gas entry to FeMo-cofactor. Recent X-ray structures of the gas utilizing hydrogenase (H_2) (Montet *et al.*, 1997) and carbon monoxide dehydrogenase (CO) (Doukov *et al.*, 2002) have revealed hydrophobic channels (without water) that connect the surface to

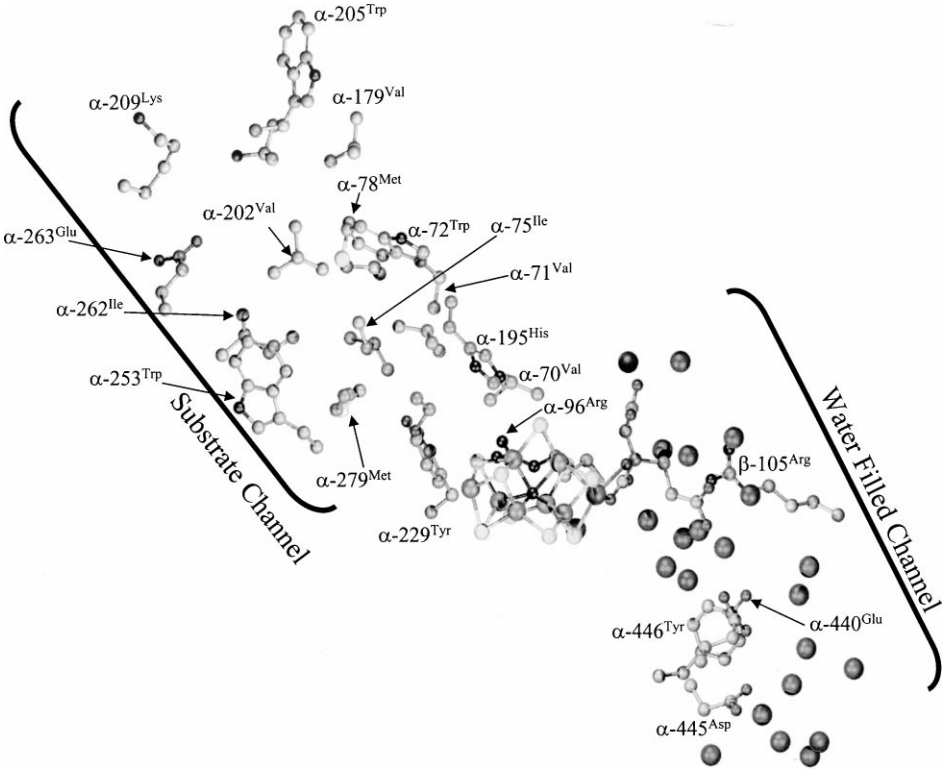

FIGURE 12. Substrate Channels. Putative gas substrate channel (top) and water filled channel (bottom) in the MoFe protein. The putative gas channel was identified using the computer program CAVENV with a 2.5 Å probe sphere. Water molecules are shown as darker spheres. The figure was generated from the PBD file 1M1N.

the active metal clusters or connect between metal clusters within the protein. It has been suggested that all gas utilizing enzymes will have such hydrophobic channels for gas movement to the metal cluster. In light of this hypothesis, and the fact that nitrogenase is a gas-utilizing enzyme, we looked for a hydrophobic channel that connects the surface to FeMo-cofactor. Using the program CAVENV from the CCP4 suite of computer programs, and a 2.5 Å probe sphere, a candidate hydrophobic channel was identified (Figure 12, top). This analysis was done in collaboration with Tzanko Doukov and Catherine Drennan (MIT). The channel is composed of three sets of amino acid residues. Near the entry point at the surface are a series of hydrophilic residues. The central portion of the channel is defined by a number of hydrophobic amino acids that lack bound water molecules. Interestingly, this putative channel leads to the Fe-S face of FeMo-cofactor that we have identified as the substrate binding site, and includes α-70^{Val}, α-195^{His}, and α-96^{Arg}.

Thus, an attractive model is that gaseous substrates enter through the gas channel to the active face of FeMo-cofactor, and that protons enter through one or more different channels. Finally, reduction products (*e.g.*, NH_4^+) would exit through the water filled channel. Experimental evidence to support this working model is clearly needed.

F. Future Prospects

This review has highlighted some of the most recent work in understanding the mechanistic steps involved in the complex metalloenzyme nitrogenase. It is apparent that significant progress has been made in many areas. In some cases, this progress has provided details of the mechanism, while in other areas, significant new results are needed. Among the areas that continue to need significant new study are:

- How is MgATP hydrolysis activated in the Fe protein when the MoFe protein docks?
- How does MgATP binding or its hydrolysis accelerate electron transfer from the Fe protein to the MoFe protein?
- Why can only the Fe protein reduce MoFe protein to support substrate reduction?

- What is the role of the P-clusters in the mechanism?
- What are the steps that occur during substrate reduction?

Progress over the next several years promises to address many of these open questions about the nitrogenase mechanism.

ACKNOWLEDGMENTS

The authors wish to acknowledge the long standing collaboration between our group and the group of Dr. Dennis Dean at Virginia Tech University on elucidating the nitrogenase mechanism. Generous support from the National Institutes of Health is gratefully acknowledged.

REFERENCES

Allen, R.M., Chatterjee, R., Madden, M.S., Ludden, P.W., and Shah, V.K. 1994. Biosynthesis of the iron-molybdenum cofactor of nitrogenase. *Crit Rev Biotech* **14:**225–249.

Andersen, J.P. and Sorensen, T. 1996. Site-directed mutagenesis studies of energy coupling in the sarcoplasmic reticulum Ca(2+)-ATPase. *Biochim Biophys Acta* **1275:**118–122.

Angove, H.C., Yoo, S.J., Burgess, B.K., and Münck, E. 1997. Mössbauer and EPR evidence for an all-ferrous Fe_4S_4 cluster with $S = 4$ in the iron protein of nitrogenase. *J Am Chem Soc* **119:**8730–8731.

Angove, H.C., Yoo, S.J., Münck, E., and Burgess, B.K. 1998. An all-ferrous state of the Fe protein of nitrogenase. Interaction with nucleotides and electron transfer to the MoFe protein. *J Biol Chem* **273:**26330–26337.

Arp, D.J. 2000. In *Prokaryotic Nitrogen Fixation*. pp. 1–14. Triplett, E. W., Ed., Horizon Scientific Press, Norfolk, England.

Benton, P.M., Christiansen, J., Dean, D.R., and Seefeldt, L.C. 2001a. Stereospecificity of acetylene reduction catalyzed by nitrogenase. *J Am Chem Soc* **123:**1822–1827.

Benton, P.M., Mayer, S.M., Shao, J., Hoffman, B.M., Dean, D.R., and Seefeldt, L.C. 2001b. Interaction of acetylene and cyanide with the resting state of nitrogenase α-96-substituted MoFe proteins. *Biochemistry* **40:**13816–13825.

Bolin, J.T., Campobasso, N., Muchmore, S.W., Morgan, T.V., and Mortenson, L.E. 1993. In *Molybdenum Enzymes, Cofactors, and Model Systems*. pp. 186–95. Steifel, E.I., Coucouvanis, D., and Newton, W.E., Eds., ACS, Washington, DC.

Bui, P.T. and Mortenson, L.E. 1968. Mechanism of the enzymatic reduction of N_2: the binding of adenosine 5′-triphosphate and cyanide to the N_2 reducing system. *Proc Natl Acad Sci USA* **61:**1021–1027.

Burgess, B.K. 1985. In *Molybdenum Enzymes*. pp. 89–116. Spiro, T.G., Ed., Wiley-Interscience, New York.

Burgess, B.K. and Lowe, D.J. 1996. Mechanism of molybdenum nitrogenase. *Chem Rev* **96:**2983–3012.

Cameron, L.M. and Hales, B.J. 1998. Investigation of CO binding and release from Mo-nitrogenase during catalytic turnover. *Biochemistry* **37:**9449–9456.

Chan, J.M., Christiansen, J., Dean, D.R., and Seefeldt, L.C. 1999a. Spectroscopic evidence for changes in the redox state of the nitrogenase P-cluster during turnover. *Biochemistry* **38:**5779–5785.

Chan, J.M., Ryle, M.J., and Seefeldt, L.C. 1999b. Evidence that MgATP accelerates primary electron transfer in a *Clostridium pasteurianum* Fe protein-*Azotobacter vinelandii* MoFe protein nitrogenase tight complex. *J Biol Chem* **274:**17593–17598.

Chan, M.K., Kim, J., and Rees, D.C. 1993. The nitrogenase FeMo-cofactor and P-cluster pair: 2.2 Å resolution structures. *Science* **260:**792–794.

Chatelet, C. and Meyer, J. 2001. Mapping the interaction of the [2Fe-2S] *Clostridium pasteurianum* ferredoxin with nitrogenase MoFe protein. *Biochim Biophys Acta* **1549:**32–36.

Chen, L., Gavini, N., Tsuruta, H., Eliezer, D., Burgess, B.K., Doniach, S., and Hodgson, K.O. 1994. MgATP-induced conformational changes in the iron protein from *Azotobacter vinelandii*, as studied by small-angle x-ray scattering. *J Biol Chem* **269:**3290–3294.

Chiu, H., Peters, J.W., Lanzilotta, W.N., Ryle, M.J., Seefeldt, L.C., Howard, J.B., and Rees, D.C. 2001. MgATP-Bound and nucleotide-free structures of a nitrogenase protein complex between the Leu 127 Δ-Fe-protein and the MoFe-protein. *Biochemistry* **40:**641–650.

Christiansen, J., Cash, V.L., Seefeldt, L.C., and Dean, D.R. 2000a. Isolation and characterization of an acetylene-resistant nitrogenase. *J Biol Chem* **275:**11459–11464.

Christiansen, J., Chan, J.M., Seefeldt, L.C., and Dean, D.R. 2000b. The role of the MoFe protein α-125^{Phe}

and β-125^{Phe} residues in *Azotobacter vinelandii* MoFe protein-Fe protein interaction. *J Inorg Biochem* **80:**195–204.

Christiansen, J., Chan, J.M., Seefeldt, L.C., and Dean, D.R. 2000c. In *Prokaryotic Nitrogen Fixation*. pp. 101–112. Triplett, E.W., Ed., Horizon Scientific Press, Norfolk, England.

Christiansen, J., Goodwin, P.J., Lanzilotta, W.N., Seefeldt, L.C., and Dean, D.R. 1998. Catalytic and biophysical properties of a nitrogenase Apo-MoFe protein produced by a *nif*B-deletion mutant of *Azotobacter vinelandii*. *Biochemistry* **37:**12611–12623.

Christiansen, J., Tittsworth, R.C., Hales, B.J., and Cramer, S.P. 1995. Fe and Mo EXAFS of *Azotobacter vinelandii* nitrogenase in partially oxidized and singly reduced forms. *J Am Chem Soc* **117:**10017–10024.

Clarke, T.A., Maritano, S., and Eady, R.R. 2000. Formation of a tight 1:1 complex of Clostridium pasteurianum Fe protein-*Azotobacter vinelandii* MoFe protein: evidence for long-range interactions between the Fe protein binding sites during catalytic hydrogen evolution. *Biochemistry* **39:**11434–11440.

Clarke, T.A., Yousafzai, F.K., and Eady, R.R. 1999. *Klebsiella pneumoniae* nitrogenase: formation and stability of putative beryllium fluoride-ADP transition state complexes. *Biochemistry* **38:**9906–9913.

Cordewener, J., Asbroek, A.T., Wassink, H., Eady, R.R., Haaker, H., and Veeger, C. 1987. Binding of ADP and orthophosphate during the ATPase reaction of nitrogenase. *Biochem J* **162:**265–270.

Cordewener, J., Haaker, H., Van Ewijk, P., and Veeger, C. 1985. Properties of the MgATP and MgADP binding sites on the Fe protein of nitrogenase from *Azotobacter vinelandii*. *Eur J Biochem* **148:**499–508.

Cordewener, J., Kruse-Wolters, M., Wassink, H., Haaker, H., and Veeger, C. 1988. The role of MgATP hydrolysis in nitrogenase catalysis. *Eur J Biochem* **172:**739–745.

Dance, I. 1996. Theoretical investigations of the mechanism of biological nitrogen fixation at the FeMo cluster site. *J Biol Inorg Chem* **1:**581–586.

Dance, I. 1997. Calculated details of a mechanism for conversion of N_2 to NH_3 at the FeMo cluster of nitrogenase. *Chem Commun* 165–166.

Dance, I. 2003. The consequences of an interstitial N atom in the FeMo cofactor of nitrogenase. *Chem Commun* **2003:**324–325.

Davidson, V.L. 2000. What controls the rates of interprotein electron-transfer reactions. *Acc Chem Res* **33:**87–93.

Davidson, V.L. 2002. Chemically gated electron transfer. A means of accelerating and regulating rates of biological electron transfer. *Biochemistry* **41:**14633–14636.

Davis, L.C., Henzl, M.T., Burris, R.H., and Orme-Johnson, W.H. 1979. Iron-sulfur clusters in the molybdenum-iron protein component of nitrogenase. Electron paramagnetic resonance of the carbon monoxide inhibited state. *Biochemistry* **18:**4860–4869.

Davis, L.C. and Orme-Johnson, W. H. 1976. Nitrogenase IX. Effect of the MgATP generator on the catalytic and EPR properties of the enzyme in vitro. *Biochim Biophys Acta* **452:**42–58.

Dean, D.R. and Jacobson, M.R. 1991. In *Biological Nitrogen Fixation*. pp. 763–834. Stacey, G., Burris, R.H., and Evans, H.J., Eds., Chapman Hall, New York.

Deits, T.L. and Howard, J.B. 1989. Kinetics of MgATP-dependent iron chelation from the Fe-protein of the *Azotobacter vinelandii* nitrogenase complex. *J Biol Chem* **264:**6619–6628.

Dilworth, M.J. 1966. Acetylene reduction by nitrogen-fixing preparations from *Clostridium pasteurianum*. *Biochim Biophys Acta* **127:**285–294.

Doukov, T.I., Iverson, T.M., Seravalli, J., Ragsdale, S.W., and Drennan, C.L. 2002. A Ni-Fe-Cu center in a bifunctional carbon monoxide dehydrogenase/acetyl-CoA synthase. *Science* **298:**567–572.

Durrant, M.C. 2002a. An atomic-level mechanism for molybdenum nitrogenase. Part 1. Reduction of dinitrogen. *Biochemistry* **41:**13934–13945.

Durrant, M.C. 2002b. An atomic-level mechanism for molybdenum nitrogenase. Part 2. Proton reduction, inhibition of dinitrogen reduction by dihydrogen, and the HD formation reaction. *Biochemistry* **41:**13946–13955.

Dutton, P.L. 1996. In *Protein Electron Transfer*. pp. 1–18. Bendall, D. S., Ed., Bios Scientific Publishers Ltd, Guildford, UK.

Duyvis, M.G., Mensink, R.E., Wassink, H., and Haaker, H. 1997. Evidence for multiple steps in the pre-steady-state electron transfer reaction of nitrogenase from *Azotobacter vinelandii*. *Biochim Biophys Acta* **1320:**34–44.

Duyvis, M.G., Wassink, H., and Haaker, H. 1996a. Formation and characterization of a transition state

complex of *Azotobacter vinelandii* nitrogenase. *FEBS Lett* **380:**233–236.

Duyvis, M.G., Wassink, H., and Haaker, H. 1996b. Pre-steady-state kinetics of nitrogenase from *Azotobacter vinelandii*. Evidence for an ATP-induced conformational change of the nitrogenase complex as part of the reaction mechanism. *J Biol Chem* **271:**29632–29636.

Duyvis, M.G., Wassink, H., and Haaker, H. 1998. Nitrogenase of *Azotobacter vinelandii*: Kinetic analysis of the Fe protein redox cycle. *Biochemistry* **37:**17345–17354.

Eady, R.R. 1996. Structure-function relationships of alternative nitrogenases. *Chem Rev* **96:**3013–3030.

Einsle, O., Texcan, F.A., Andrade, S.L.A., Schmid, B., Yoshida, M., Howard, J.B., and Rees, D.C. 2002. Nitrogenase MoFe-protein at 1.16 Å resolution: A central ligand in the FeMo-cofactor. *Science* **297:**1696–1700.

Emerich, D.W. and Burris, R.H. 1976. Interactions of heterologous nitrogenase components that generate catalytically inactive complexes. *Proc Natl Acad Sci USA* **73:**4369–4373.

Emerich, D.W. and Burris, R.H. 1978. Complementary functioning of the component proteins of nitrogenase from several bacteria. *J Bacteriol* **134:**936–943.

Emerich, D.W., Ljones, T., and Burris, R.H. 1978. Nitrogenase: Properties of the catalytically inactive complex between the *Azotobacter vinelandii* MoFe protein and the *Clostridium pasteurianum* Fe protein. *Biochem Biophys Acta* **527:**359–369.

Ferguson, S.J. 1998. Nitrogen cycle enzymology. *Curr Opin Chem Biol* **2:**182–193.

Finan, T.M., O'Brian, M.R., Lazell, D.B., Vessey, J.K., and Newton, W.E. 2002. In *Nitrogen Fixation, Proc. Int. Congr., 13th, 2002. Nitrogen Fixation: Global Perspectives (Proceedings of the 13th International Congress held 2–7 July 2001 in Ontario, Canada.)* CABI Publishing, Wallingford, UK.

Fisher, K., Dilworth, M.J., Kim, C.H., and Newton, W.E. 2000a. *Azotobacter vinelandii* nitrogenases containing altered MoFe proteins with substitutions in the FeMo-cofactor environment: Effects on the catalyzed reduction of acetylene and ethylene. *Biochemistry* **39:**2970–2979.

Fisher, K., Dilworth, M.J., Kim, C.H., and Newton, W.E. 2000b. *Azotobacter vinelandii* nitrogenases with substitutions in the FeMo- cofactor environment of the MoFe protein: Effects of acetylene or ethylene on interactions with H+, HCN, and CN. *Biochemistry* **39:**10855–10865.

Fisher, K., Dilworth, M.J., and Newton, W.E. 2000c. Differential effects on N_2 binding and reduction, HD formation, and azide reduction with α-195^{His}- and α-191^{Gln}-substituted MoFe proteins of *Azotobacter vinelandii* nitrogenase. *Biochemistry* **39:**15570–15577.

Fu, W.G., Morgan, T.V., Mortenson, L.E., and Johnson, M.K. 1991. Resonance Raman studies of the [4Fe-4S] to [2Fe-2S] cluster conversion in the iron protein of nitrogenase. *FEBS Lett* **284:**165–168.

Gavini, N., Ma, L., Watt, G., and Burgess, B.K. 1994. Purification and characterization of a FeMo cofactor-deficient MoFe protein. *Biochemistry* **33:**11842–11849.

Georgiadis, M.M., Komiya, H., Chakrabarti, P., Woo, D., Kornuc, J.J., and Rees, D.C. 1992. Crystallographic structure of the nitrogenase iron protein from *Azotobacter vinelandii*. *Science* **257:**1653–1659.

Gray, H.B. and Winkler, J.R. 1996. Electron transfer in proteins. *Annu Rev Biochem* **65:**537–561.

Grönberg, K.L.C., Gormal, C.A., Durrant, M.C., Smith, B.E., and Henderson, R.A. 1998. Why *R*-homocitrate is essential to the reactivity of FeMo-cofactor of nitrogenase: Studies on NifV$^-$-extracted FeMo-cofactor. *J Am Chem Soc* **120:**10613–10621.

Grossman, J.G., Hasnain, S.S., Yousafzai, F.K., Smith, B.E., and Eady, R.R. 1997. The first glimpse of a complex of nitrogenase component proteins by solution X-ray scattering: Conformation of the electron transfer transition state complex of *Klebsiella pneumoniae* nitrogenase. *J Mol Biol* **266:**642–648.

Guo, M., Sulc, F., Ribbe, M.W., Farmer, P.J., and Burgess, B.K. 2002. Direct assessment of the reduction potential of the [4Fe-4S]$^{1+/0}$ couple of the Fe protein from *Azotobacter vinelandii*. *J Am Chem Soc* **124:**12100–12101.

Guth, J.H. and Burris, R.H. 1983. Inhibition of nitrogenase-catalyzed NH_3 formation by H_2. *Biochemistry* **22:**5111–5122.

Haber, F. 1922. The production of ammonia from nitrogen and hydrogen. *Naturwissenschaften* **10:**1041.

Haber, F. and Le Rossignol, R. 1908. The ammonia equilibrium under pressure. *Z Elektrochem* **14:**181.

Hadfield, K.L. and Bulen, W.A. 1969. Adenosine triphosphate requirement of nitrogenase. *Biochemistry* **8:**5103–5108.

Hageman, R.V. and Burris, R.H. 1978. Nitrogenase and nitrogenase reductase associate and dissociate with each catalytic cycle. *Proc Natl Acad Sci USA* **75:**2699–2702.

Hagen, W.R., Dunham, W.R., Braaksma, A., and Haaker, H. 1985a. On the prosthetic group(s) of component II from nitrogenase. EPR of the Fe-protein from *Azotobacter vinelandii*. *FEBS Lett* **187:**146–150.

Hagen, W.R., Eady, R.R., Dunham, W.R., and Haaker, H. 1985b. A novel $S = 3/2$ EPR signal associated with native Fe-proteins of nitrogenase. *FEBS Lett* **189:**250–254.

Hagen, W.R., Wassink, H., Eady, R.R., Smith, B.E., and Haaker, H. 1987. Quantitative EPR of an $S = 7/2$ system in thionine-oxidized MoFe proteins of nitrogenase. A redefinition of the P-cluster concept. *Eur J Biochem* **169:**457–465.

Hallenbeck, P.C. and Gennaro, G. 1998. Stopped-flow kinetic studies of low potential electron carriers of the photosynthetic bacterium, *Rhodobacter capsulatus*: Ferredoxin I and NifF. *Biochim Biophys Acta* **1365:**435–442.

Hardy, R.W., Knight, E., Jr., and D'Eustachio, A.J. 1965. An energy-dependent hydrogen-evolution from dithionite in nitrogen-fixing extracts of *Clostridium pasteurianum*. *Biochem Biophys Res Commun* **20:**539–544.

Hardy, R.W.F., Holsten, R.D., Jackson, E.K., and Burns, R.C. 1968. *Plant Physiol* **43:**1185–1207.

Hausinger, R.P. and Howard, J.B. 1982. The amino acid sequence of the nitrogenase iron protein from *Azotobacter vinelandii*. *J Biol Chem* **257:**2483–2490.

Hinnemann, B. and Norskov, J.K. 2003. Modeling a Central Ligand in the Nitrogenase FeMo Cofactor. *J Am Chem Soc* **125:**1466–1467.

Hirst, J., Duff, J.L.C., Jameson, G.N.L., Kemper, M.A., Burgess, B.K., and Armstrong, F.A. 1998. Kinetics and mechanism of redox-coupled, long-range proton transfer in an iron-sulfur protein. Investigation by fast-scan protein-film voltammetry. *J Am Chem Soc* **120:**7085–7094.

Howard, J.B. and Rees, D.C. 1994. Nitrogenase: A nucleotide-dependent molecular switch. *Annu Rev Biochem* **63:**235–264.

Hughes, D.L., Mohammed, M.Y., and Pickett, C.J. 1989. Electroreduction of co-ordinated cyanide to the aminocarbyne ligand (CNH_2) and a pathway for isomerization of ligating methyleneamide (NCH_2): Reactions at molybdenum of relevance to cyanide reduction by nitrogenase. *Chem Commun* **18:**1399–1400.

Huynh, B.H., Henzl, M.T., Christner, M.T., Zimmerman, R., Orme-Johnson, W.H., and Münck, E. 1980. Nitrogenase XII. Mössbauer studies of the MoFe Protein from *Clostridium pasteurianum* W5. *Biochem Biophys Acta* **623:**124–138.

Hwang, J.C., Chen, C.H., and Burris, R.H. 1973. Inhibition of nitrogenase-catalyzed reductions. *Biochem Biophys Acta* **292:**256–270.

Jang, S.B., Seefeldt, L.C., and Peters, J.W. 2000. Insights into nucleotide signal transduction in nitrogenase: Structure of an iron protein with MgADP bound. *Biochemistry* **39:**14745–14752.

Kelly, M. 1969. Comparisons and cross reactions of nitrogenase from *Klebsiella pneumoniae*, *Azotobacter chroococcum* and *Bacillus polymyxa*. *Biochim Biophys Acta* **191:**527–540.

Kim, C.-H., Newton, W.E., and Dean, D.R. 1995. Role of the MoFe protein α-subunit histidine-195 residue in FeMo-cofactor binding and nitrogenase catalysis. *Biochemistry* **34:**2798–2808.

Kim, J. and Rees, D.C. 1992. Structural models for the metal centers in the nitrogenase molybdenum-iron protein. *Science* **257:**1677–1682.

Kim, J., Woo, D., and Rees, D.C. 1993. X-ray crystal structure of the nitrogenase molybdenum-iron protein from *Clostridium pasteurianum* at 3.0-A resolution. *Biochemistry* **32:**7104–7115.

Kurnikov, I.V., Charnley, A.K., and Beratan, D.N. 2001. From ATP to electron transfer: Electrostatics and Free-Energy Transduction in Nitrogenase. *J Phys Chem B* **105:**5359–5367.

Langen, R., Colon, J.L., Casimiro, D.R., Danilo, R., Karpishin, T.B., Winkler, J.R., and Gray, H.B. 1996. Electron tunneling in proteins: Role of the intervening medium. *J Biol Inorg Chem* **1:**221–225.

Lanzilotta, W.N., Christiansen, J., Dean, D.R., and Seefeldt, L.C. 1998a. Evidence for coupled electron and proton transfer in the [8Fe-7S] cluster of nitrogenase. *Biochemistry* **37:**11376–11384.

Lanzilotta, W.N., Fisher, K., and Seefeldt, L.C. 1996. Evidence for electron transfer from the nitrogenase iron protein to the molybdenum-iron protein without MgATP hydrolysis: Characterization of a tight protein-protein complex. *Biochemistry* **35:**7188–7196.

Lanzilotta, W.N., Fisher, K., and Seefeldt, L.C. 1997. Evidence for electron transfer-dependent formation of a nitrogenase iron protein-molybdenum-iron protein tight complex. The role of aspartate 39. *J Biol Chem* **272:**4157–4165.

Lanzilotta, W.N., Holz, R.C., and Seefeldt, L.C. 1995a. Proton NMR investigation of the [4Fe-4S]$^{1+}$ cluster environment of nitrogenase iron protein from *Azotobacter vinelandii*: Defining nucleotide-induced conformational changes. *Biochemistry* **34:**15646–15653.

Lanzilotta, W.N., Parker, V.D., and Seefeldt, L.C. 1998b. Electron transfer in nitrogenase analyzed by Marcus theory: Evidence for gating by MgATP. *Biochemistry* **37:**399–407.

Lanzilotta, W.N., Parker, V.D., and Seefeldt, L.C. 1999. Thermodynamics of nucleotide interactions with the *Azotobacter vinelandii* nitrogenase iron protein. *Biochim Biophys Acta* **1429:**411–421.

Lanzilotta, W.N., Ryle, M.J., and Seefeldt, L.C. 1995b. Nucleotide hydrolysis and protein conformational changes in *Azotobacter vinelandii* nitrogenase iron protein: Defining the function of aspartate 129. *Biochemistry* **34:**10713–10723.

Lanzilotta, W.N. and Seefeldt, L.C. 1997. Changes in the midpoint potentials of the nitrogenase metal centers as a result of iron protein-molybdenum-iron protein complex formation. *Biochemistry* **36:**12976–12983.

Larsen, C., Christiansen, S., and Watt, G.D. 1995. Reductant-independent ATP hydrolysis catalyzed by homologous nitrogenase proteins from *Azotobacter vinelandii* and heterologous crosses with *Clostridium pasteurianum*. *Arch Biochem Biophys* **323:**215–222.

Lee, H.-I., Benton, P.M.C., Laryukhin, M., Igarashi, R.Y., Dean, D.R., Seefeldt, L.C., and Hoffman, B.M. 2003. The interstitial atom of the nitrogenase FeMo-cofactor: ENDOR and ESEEM show it is not an exchangeable nitrogen. *J Am Chem Soc* **125:**5604–5605.

Lee, H.I., Cameron, L.M., Hales, B.J., and Hoffman, B.M. 1997a. CO binding to the FeMo cofactor of CO-inhibited nitrogenase: 13CO and 1H Q-band ENDOR investigation. *J Am Chem Soc* **119:**10121–10126.

Lee, H.I., Hales, B.J., and Hoffman, B.M. 1997b. Metal-ion valencies of the FeMo cofactor in CO-inhibited and resting state nitrogenase by ^{57}Fe Q-band ENDOR. *J Am Chem Soc* **119:**11395–11400.

Lindahl, P.A., Day, E.P., Kent, T.A., Orme-Johnson, W.H., and Münck, E. 1985. Mössbauer, EPR, and magnetization studies of the *Azotobacter vinelandii* Fe protein. Evidence for a [4Fe-4S]$^{1+}$ cluster with spin $S = 3/2$. *J Biol Chem* **260:**11160–11173.

Lindahl, P.A., Papaefthymiou, V., Orme-Johnson, W.H., and Münck, E. 1988. Mössbauer studies of solid thionin-oxidized MoFe protein of nitrogenase. *J Biol Chem* **263:**19412–19418.

Lindahl, P.A., Teo, B.-K., and Orme-Johnson, W.H. 1987. EXAFS studies of the nitrogenase iron protein from *Azotobacter vinelandii*. *Inorg Chem* **26:**3912–3916.

Ljones, T. and Burris, R.H. 1978. Nitrogenase: The reaction between the Fe protein and bathophenanthrolinedisulfonate as a probe for interactions with MgATP. *Biochemistry* **17:**1866–1872.

Lovell, T., Li, J., Liu, T., Case, D.A., and Noodleman, L. 2001. FeMo cofactor of nitrogenase: A density functional study of states M^N, M^{OX}, M^R, and M^I. *J Am Chem Soc* **123:**12392–12410.

Lovell, T., Liu, T., Case, D.A., and Noodleman, L. 2003. Structural, spectroscopic, and redox consequences of a central ligand in the nitrogenase MoFe cofactor. *J Am Chem Soc* **125:**8377–8383.

Lowe, D.J. and Thorneley, R.N.F. 1984a. The mechanism of *Klebsiella pneumoniae* nitrogenase action. The determination of rate constants required for the simulation of kinetics of N_2 reduction and H_2 evolution. *Biochem J* **224:**895–901.

Lowe, D.J. and Thorneley, R.N.F. 1984b. The mechanism of *Klebsiella pneumoniae* nitrogenase action. Pre-steady-state kinetics of H_2 formation. *Biochem J* **224:**877–886.

Lowery, R.G., Chang, C.L., Davis, L.C., McKenna, M.C., Stephens, P.J., and Ludden, P.W. 1989. Substitution of histidine for arginine-101 of dinitrogenase reductase disrupts electron transfer to dinitrogenase. *Biochemistry* **28:**1206–1212.

Ma, L., Brosius, M.A., and Burgess, B.K. 1996. Construction of a form of the MoFe protein of nitrogenase that accepts electrons from the Fe protein but does not reduce substrate. *J Biol Chem* **271:**10528–10532.

Madden, M.S., Kindon, N.D., Ludden, P.W., and Shah, V.K. 1990. Diastereomer-dependent substrate reduction properties of a dinitrogenase containing 1-fluorohomocitrate in the iron-molybdenum cofactor. *Proc Natl Acad Sci USA* **87:**6517–6521.

Madden, M.S., Paustaian, T.D., Ludden, P.W., and Shah, V.K. 1991. Effects of homocitrate, homocitrate lactone, and fluorohomocitrate on nitrogenase in NifV$^-$ mutants of *Azotobacter vinelandii*. *J Bacteriol* **173:**5403–5405.

Maritano, S., Fairhurst, S.A., and Eady, R.R. 2001. Long-range interactions between the Fe protein binding sites of the MoFe protein of nitrogenase. *J Bio Inorg Chem* **2001:**590–600.

Maskos, Z. and Hales, B.J. 2003. Photo-lability of CO bound to Mo-nitrogenase from *Azotobacter vinelandii*. *J Inorg Biochem* **93:**11–17.

Mayer, S.M., Lawson, D.M., Gormal, C.A., Roe, S.M., and Smith, B.E. 1999. New insights into structure-function relationships in nitrogenase: A 1.6 Å resolution X-ray crystallographic study of *Klebsiella pneumoniae* MoFe-protein. *J Mol Biol* **292:**871–891.

Mayer, S.M., Niehaus, W.G., and Dean, D.R. 2002. Reduction of short chain alkynes by a nitrogenase α-70^{Ala}-substituted MoFe protein. *Dalton Trans* **2002:**802–807.

Meyer, J., Gaillard, J., and Moulis, J.M. 1988. Hydrogen-1 nuclear magnetic resonance of the nitrogenase iron protein (Cp2) from *Clostridium pasteurianum*. *Biochemistry* **27:**6150–6156.

Miller, R.W., Eady, R.R., Fairhurst, S.A., Gormal, C.A., and Smith, B.E. 2001. Transition state complexes of the *Klebsiella pneumoniae* nitrogenase proteins. Spectroscopic properties of aluminium fluoride-stabilized and beryllium fluoride-stabilized MgADP complexes reveal conformational differences of the Fe protein. *Eur J Biochem* **268:**809–818.

Montet, Y., Amara, P., Volbeda, A., Vernede, X., Hatchikian, E.C., Field, M.J., Frey, M., and Fontecilla-Camps, J.C. 1997. Gas access to the active site of Ni-Fe hydrogenases probed by X-ray crystallography and molecular dynamics. *Nat Struct Biol* **4:**523–526.

Morgan, T.V., McCracken, J., Orme-Johnson, W.H., Mims, W.B., Mortenson, L.E., and Peisach, J. 1990. Pulsed electron paramagnetic resonance studies of the interaction of Mg-ATP and D_2O with the iron protein of nitrogenase. *Biochemistry* **29:**3077–3082.

Morgan, T.V., Mortenson, L.E., McDonald, J.W., and Watt, G.D. 1988. Comparison of redox and EPR properties of the molybdenum iron proteins of *Clostridium pasteurianum* and *Azotobacter vinelandii* nitrogenases. *J Inorg Biochem* **33:**111–120.

Mortenson, L.E. 1964. Ferredoxin and adenosine triphosphate (ATP) requirements for N fixation in cell-free extracts of *Clostridium pasteurianum*. *Proc Natl Acad Sci USA* **52:**272–279.

Mortenson, L.E., Seefeldt, L.C., Morgan, T.V., and Bolin, J.T. 1993. In *Advances in Enzymology*. pp. 299–374. Meister, A., Ed., John Wiley and Sons, Inc., New York.

Mortenson, L.E., Webb, M., Bare, R., Cramer, S.P., and Morgan, T.V. 1985. In *Nitrogen Fixation Research Progress*. pp. 577–583. Evans, H.J., Bottomley, P.J., and Newton, W.E., Eds., Nijhoff, Dordrecht, The Netherlands.

Mortenson, L.E., Zumft, W.G., and Palmer, G. 1973. Electron paramagnetic resonance studies on nitrogenase III. Function of magnesium adenosine 5'-triphosphate and adenosine 5′-diphosphate in catalysis by nitrogenase. *Biochem Biophys Acta* **292:**422–435.

Mouesca, J.-M., Noodleman, L., and Case, D.A. 1994. Analysis of the ^{57}Fe hyperfine coupling constants and spin states in nitrogenase P-clusters. *Inorg Chem* **33:**4819–4830.

Moustafa, E. and Mortenson, L.E. 1967. Acetylene reduction by nitrogen fixing extracts of *Clostridium pasteurianum*: ATP requirement and inhibition by ADP. *Nature* **216:**1241–1242.

Musgrave, K.B., Angove, H.C., Burgess, B.K., Hedman, B., and Hodgson, K.O. 1998. All-ferrous titanium(III) citrate reduced Fe protein of nitrogenase: An XAS study of electronic and metrical structure. *J Am Chem Soc* **120:**5325–5326.

O'Donnell, M.J. and Smith, B.E. 1978. Electron-paramagnetic-resonance studies on the redox properties of the molybdenum-iron protein of nitrogenase between +50 and −450 mV. *Biochem J* **173:**831–839.

Orme-Johnson, W.H., Hamilton, W.D., Jones, T.L., Tso, M.Y., Burris, R.H., Shah, V.K., and Brill, W.J. 1972. Electron paramagnetic resonance of nitrogenase and nitrogenase components from *Clostridium pasteurianum* W5 and *Azotobacter vinelandii* OP. *Proc Natl Acad Sci USA* **69:**3142–3145.

Peters, J.W., Fisher, K., and Dean, D.R. 1994. Identification of a nitrogenase protein-protein interaction site defined by residues 59 through 67 within the *Azotobacter vinelandii* Fe protein. *J Biol Chem* **269:**28076–28083.

Peters, J.W., Stowell, M.H., Soltis, S.M., Finnegan, M.G., Johnson, M.K., and Rees, D.C. 1997. Redox-dependent structural changes in the nitrogenase P-cluster. *Biochemistry* **36:**1181–1187.

Pickett, C.J. 1996. The Chatt cycle and the mechanism of enzymic reduction of molecular nitrogen. *J Bio Inorg Chem* **1:**601–606.

Pickett, C.J., Vincent, K.A., Ibrahim, S.K., Gormal, C.A., Smith, B.E., and Best, S.P. 2003. Electron-transfer chemistry of the iron-molybdenum cofactor of nitrogenase: Delocalized and localized reduced states of FeMoco which allow binding of carbon

monoxide to iron and molybdenum. *Chemistry* **9:**76–87.

Pierik, A.J., Wassink, H., Haaker, H., and Hagen, W.R. 1993. Redox properties and EPR spectroscopy of the P clusters of *Azotobacter vinelandii* MoFe protein. *Eur J Biochem* **212:**51–61.

Pollock, R.C., Lee, H.I., Cameron, L.M., DeRose, V.J., Hales, B.J., Orme-Johnson, W.H., and Hoffman, B.M. 1995. Investigations of CO bound inhibited forms of nitrogenase MoFe protein by ^{13}C ENDOR. *J Am Chem Soc* **117:**8686–8687.

Rees, D.C., Schindelin, H., Kisker, C., Schlessman, J., Peters, J.W., Seefeldt, L.C., and Howard, J.B. 1998. Complex structures of nitrogenase. *Curr Plant Sci Biotech Ag* **31:**11–16.

Rehder, D., Bashirpoor, M., Jantzen, S., Schmidt, H., Farahbakahsh, M., and Nekola, H. 1998. Structural and functional models for biogenic vanadium compounds. *ACS Symposium Series* **711:**60–70.

Renner, K.A. and Howard, J.B. 1996. Aluminum fluoride inhibition of nitrogenase: Stabilization of a nucleotide·Fe-protein·MoFe-protein complex. *Biochemistry* **35:**5353–5358.

Ribbe, M., Gadkari, D., and Meyer, O. 1997. N_2 fixation by *Streptomyces thermoautotrophicus* involves a molybdenum-dinitrogenase and a manganese-superoxide oxidoreductase that couple N_2 reduction to the oxidation of superoxide produced from O_2 by a molybdenum-CO dehydrogenase. *J Biol Chem* **272:**26627–26633.

Ribbe, M.W., Hu, Y., Guo, M., Schmid, B., and Burgess, B.K. 2002. The FeMoco-deficient MoFe protein produced by a *nif*H deletion strain of *Azotobacter vinelandii* shows unusual P-cluster features. *J Biol Chem* **277:**23469–23476.

Rivera-Ortiz, J.M. 1975. Interactions among substrate and inhibitors of nitrogenase. *J Bacteriol* **123:**537–545.

Rod, T.H., Hammer, B., and Norskov, J.K. 1999. Nitrogen adsorption and hydrogenation on a $MoFe_6S_9$ complex. *Phys Rev Lett* **82:**4054–4057.

Rod, T.H. and Norskov, J.K. 2000. Modeling the nitrogenase FeMo cofactor. *J Am Chem Soc* **122:**12751–12763.

Ruttimann-Johnson, C., Chatterjee, R., Shah, V.K., and Ludden, P.W. 1998. The vanadium-containing nitrogenase system of *Azotobacter vinelandii*. *ACS Symposium Series* **711:**228–240.

Ryle, M.J., Lanzilotta, W.N., Mortenson, L.E., Watt, G.D., and Seefeldt, L.C. 1995. Evidence for a central role of lysine 15 of *Azotobacter vinelandii* nitrogenase iron protein in nucleotide binding and protein conformational changes. *J Biol Chem* **270:**13112–13117.

Ryle, M.J., Lanzilotta, W.N., and Seefeldt, L.C. 1996a. Elucidating the mechanism of nucleotide-dependent changes in the redox potential of the [4Fe-4S] cluster in nitrogenase iron protein: The role of phenylalanine 135. *Biochemistry* **35:**9424–9434.

Ryle, M.J., Lanzilotta, W.N., Seefeldt, L.C., Scarrow, R.C., and Jensen, G.M. 1996b. Circular dichroism and x-ray spectroscopies of *Azotobacter vinelandii* nitrogenase iron protein. MgATP and MgADP induced protein conformational changes affecting the [4Fe-4S] cluster and characterization of a [2Fe-2S] form. *J Biol Chem* **271:**1551–1557.

Ryle, M.J., Lee, H.I., Seefeldt, L.C., and Hoffman, B.M. 2000. Nitrogenase reduction of carbon disulfide: Freeze-quench EPR and ENDOR evidence for three sequential intermediates with cluster-bound carbon moieties. *Biochemistry* **39:**1114–1119.

Ryle, M.J. and Seefeldt, L.C. 1996. Elucidation of a MgATP signal transduction pathway in the nitrogenase iron protein: Formation of a conformation resembling the MgATP-bound state by protein engineering. *Biochemistry* **35:**4766–4775.

Schindelin, H., Kisker, C., Schlessman, J.L., Howard, J.B., and Rees, D.C. 1997. Structure of ADP x AlF_4^--stabilized nitrogenase complex and its implications for signal transduction. *Nature* **387:**370–376.

Schmitz, R.A., Klopprogge, K., and Grabbe, R. 2002. Regulation of nitrogen fixation in *Klebsiella pneumoniae* and *Azotobacter vinelandii*: NifL, transducing two environmental signals to the *nif* transcriptional activator NifA. *J Mol Biol and Biotech* **4:**225–242.

Schultz, F.A., Gheller, S.F., and Newton, W.E. 1988. Iron-molybdenum cofactor of nitrogenase: Electrochemical determination of the electron stoichiometry of the oxidized/semi-reduced couple. *Biochem Biophys Res Commun* **152:**629–635.

Seefeldt, L.C. 1994. Docking of nitrogenase iron- and molybdenum-iron proteins for electron transfer and MgATP hydrolysis: The role of arginine 140 and lysine 143 of the *Azotobacter vinelandii* iron protein. *Protein Sci* **3:**2073–2081.

Siegbahn, P.E.M. and Blomberg, M.R.A. 1999. Density functional theory of biologically relevant metal centers. *Annu Rev Phys Chem* **50:**221–249.

Siegbahn, P.E.M., Westerberg, J., Svensson, M., and Crabtree, R.H. 1998. Nitrogen fixation by

nitrogenases: A quantum chemical study. *J Phys Chem B* **102:**1615–1623.

Simpson, F.B. and Burris, R.H. 1984. A nitrogen pressure of 50 atmospheres does not prevent evolution of hydrogen by nitrogenase. *Science* **224:**1095–1097.

Smil, V. 2001. In *Enriching the Earth: Fritz Haber, Carl Bosch, and the Transformation of World Food Production*. The MIT Press, Cambridge, MA.

Smith, B.E. 1999. Structure, function, and biosynthesis of the metallosulfur clusters in nitrogenases. *Adv Inorg Chem* **47:**159–218.

Smith, B.E., Durrant, M.C., Fairhurst, S.A., Gormal, C.A., Grönberg, K.L.C., Henderson, R.A., Ibrahim, S.K., Gall, T.L., and Pickett, C.J. 1999. Exploring the reactivity of the isolated iron-molybdenum cofactor of nitrogenase. *Coord Chem Rev* **185-186:**669–687.

Smith, B.E., Lowe, D.J., and Bray, R.C. 1973. Studies by electron paramagnetic resonance on the catalytic mechanism of nitrogenase of *Klebsiella pneumoniae*. *Biochem J* **135:**331–341.

Sorlie, M., Christiansen, J., Dean, D.R., and Hales, B.J. 1999. Detection of a new radical and FeMo-Cofactor EPR signal during acetylene reduction by the α-H195Q mutant of nitrogenase. *J Am Chem Soc* **121:**9457–9458.

Sorlie, M., Christiansen, J., Lemon, B.J., Peters, J.W., Dean, D.R., and Hales, B.J. 2001. Mechanistic features and structure of the nitrogenase α-Gln^{195} MoFe protein. *Biochemistry* **40:**1540–1549.

Spee, J.H., Arendsen, A.F., Wassink, H., Marritt, S.J., Hagen, W.R., and Haaker, H. 1998. Redox properties and electron paramagnetic resonance spectroscopy of the transition state complex of *Azotobacter vinelandii* nitrogenase. *FEBS Lett* **432:** 55–58.

Strop, P., Takahara, P.M., Chiu, H., Angove, H.C., Burgess, B.K., and Rees, D.C. 2001. Crystal structure of the all-ferrous $[4Fe\text{-}4S]^0$ form of the nitrogenase iron protein from *Azotobacter vinelandii*. *Biochemistry* **40:**651–656.

Sun, D. and Davidson, V.L. 2002. Mechanism of catalysis and electron transfer by tryptophan tryptophylquinone enzymes. *Prog React Kinet Mech* **27:**209–241.

Surerus, K.K., Hendrich, M.P., Christie, P.D., Tottgardt, D., Orme-Johnson, W.H., and Münck, E. 1992. Mössbauer and integer-spin EPR of the oxidized P-cluster of nitrogenase: P^{ox} is a non-Kramers system with a nearly degenerate ground doublet. *J Am Chem Soc* **114:**8579–8590.

Thorneley, R.N.F. and Ashby, G.A. 1989. Oxidation of nitrogenase iron protein by dioxygen without inactivation could contribute to high respiration rates of *Azotobacter* species and facilitate nitrogen fixation in other aerobic environments. *Biochem J* **261:**181–187.

Thorneley, R.N.F., Eady, R.R., and Lowe, D.J. 1978. Biological nitrogen fixation by way of an enzyme-bound dinitrogen-hydride intermediate. *Nature* **272:**557–558.

Thorneley, R.N.F. and Lowe, D.J. 1983. Nitrogenase of *Klebsiella pneumoniae*, kinetics of the dissociation of oxidized iron protein from molybdenum-iron protein: Identification of the rate-limiting step for substrate reduction. *Biochem J* **215:**393–403.

Thorneley, R.N.F. and Lowe, D.J. 1984a. The mechanism of *Klebsiella pneumoniae* nitrogenase action. Pre-steady-state kinetics of an enzyme-bound intermediate in N_2 reduction and of NH_3 formation. *Biochem J* **224:**887–894.

Thorneley, R.N.F. and Lowe, D.J. 1984b. The mechanism of Klebsiella pneumoniae nitrogenase action. Simulation of the dependences of H_2-evolution rate on component-protein concentration and ratio and sodium dithionite concentration. *Biochem J* **224:**903–909.

Thorneley, R.N.F. and Lowe, D.J. 1985. In *Molybdenum Enzymes*. pp. 89–116. Spiro, T.G., Ed., Wiley-Interscience, New York.

Tittsworth, R.C. and Hales, B.J. 1993. Detection of EPR signals assigned to the 1-equivalence-oxidized P-cluster of the nitrogenase MoFe-protein from *Azotobacter vinelandii*. *J Am Chem Soc* **115:**9763–9767.

Torres, R.A., Lovell, T., Noodleman, L., and Case, D.A. 2003. Density functional and reduction potential calculations of Fe4S4 clusters. *J Am Chem Soc* **125:**1923–1936.

Walker, G.A. and Mortenson, L.E. 1974. Effect of magnesium adenosine 5′-triphosphate on the accessibility of the iron of clostridial azoferredoxin, a component of nitrogenase. *Biochemistry* **13:**2382–2388.

Watt, G.D. 1979. An electrochemical method for measuring redox potentials of low potential proteins by microcoulometry at controlled potentials. *Anal Biochem* **99:**399–407.

Watt, G.D., Burns, A., Lough, S., and Tennent, D.L. 1980. Redox and spectroscopic properties of oxidized MoFe Protein from *Azotobacter vinelandii*. *Biochemistry* **19:**4926–4932.

Watt, G.D. and Reddy, K.R.N. 1994. Formation of an all ferrous Fe_4S_4 cluster in the iron protein component of *Azotobacter vinelandii* nitrogenase. *J Inorg Biochem* **53:**281–294.

Watt, G.D., Wang, A.-C., and Knotts, R.R. 1986. Redox reactions of and nucleotide binding to the iron protein of *Azotobacter vinelandii*. *Biochemistry* **25:**8156–8162.

Weston, M.F., Kotake, S., and Davis, L.C. 1983. Interaction of nitrogenase with nucleotide analogs of ATP and ADP and the effect of metal ions on ADP inhibition. *Arch Biochem Biophys* **225:**809–817.

Willing, A. and Howard, J.B. 1990. Cross-linking site in *Azotobacter vinelandii* complex. *J Biol Chem* **265:**6596–6599.

Willing, A.H., Georgiadis, M.M., Rees, D.C., and Howard, J.B. 1989. Cross-linking of nitrogenase components. Structure and activity of the covalent complex. *J Biol Chem* **264:**8499–8503.

Wilson, P.E., Nyborg, A.C., and Watt, G.D. 2001. Duplication and extension of the Thorneley and Lowe kinetic model for *Klebsiella pneumoniae* nitrogenase catalysis using a MATHEMATICA software platform. *Biophys Chem* **91:**281–304.

Wolle, D., Kim, C., Dean, D., and Howard, J.B. 1992. Ionic interactions in the nitrogenase complex. Properties of Fe-protein containing substitutions for Arg-100. *J Biol Chem* **267:**3667–3673.

Yates, M.G. 1992. The enzymology of molybdenum-dependent nitrogen fixation. In *Biological Nitrogen Fixation*. pp. 686–735. Stacey, G., Burris, R.H., and Evans, H.J., Eds., Chapman & Hall, New York.

Yoo, S.J., Angove, H.C., Burgess, B.K., Münck, E., and Peterson, J. 1998. Magnetic circular dichroism study of the all-ferrous [4Fe-4S] cluster of the Fe-protein of *Azotobacter vinelandii* nitrogenase. *J Am Chem Soc* **120:**9704–9705.

Yoo, S.J., Angove, H.C., Papaefthymiou, V., Burgess, B.K., and Münck, E. 2000. Mössbauer study of the MoFe protein of nitrogenase from *Azotobacter vinelandii* using selective ^{57}Fe enrichment of the M-centers. *J Am Chem Soc* **122:**4926–4936.

Zimmermann, R., Münck, E., Brill, W.J., Shah, V.K., Henzl, M.T., Rawlings, J., and Orme-Johnson, W.H. 1978. Nitrogenase X: Mössbauer and EPR studies on reversibly oxidized MoFe protein from *Azotobacter vinelandii* OP. Nature of the iron centers. *Biochem Biophys Acta* **537:**185–207.

Zumft, W.G. 1997. Cell biology and molecular basis of denitrification. *Microbiol Mol Biol Rev* **61:**533–616.

Zumft, W.G., Mortenson, L.E., and Palmer, G. 1974. Electron-paramagnetic-resonance studies on nitrogenase. Investigation of the oxidation-reduction behaviour or azoferredoxin and molybdoferredoxin with potentiometric and rapid-freeze techniques. *Eur J Biochem* **46:**525–535.

Zumft, W.G., Palmer, G., and Mortenson, L.E. 1973. Electron paramagnetic resonance studies on nitrogenase. II. Interaction of adenosine 5′-triphosphate with azoferredoxin. *Biochim Biophys Acta* **292:**413–421.